Experimental study of the effect of increased CO_2 concentration on infrared radiation absorption

Jan Kubicki
Tomasz Wójcik

WUST Publishing House

Jan Kubicki
Tomasz Wójcik

Experimental study of the effect of increased CO_2 concentration on infrared radiation absorption

WUST Publishing House
Wrocław 2026

Reviewers
Mariusz BŁOCHOWIAK
Edward PLIŃSKI

Linguistic verification
Jolanta WRÓBEL

Technical editor
Stanisław GANCARZ

Cover design
Janusz M. SZAFRAN

WUST Publishing House
Wybrzeże Wyspiańskiego 27, 50-370 Wrocław
http://www.oficyna.pwr.edu.pl
e-mail: oficwyd@pwr.edu.pl
zamawianie.ksiazek@pwr.edu.pl

ISBN 978-83-8134-019-9
DOI: 10.37190/J-Kubicki_T-Wojcik_2026

Print and binding: beta-druk, www.betadruk.pl

Contents

1. Introduction

The foundation of the so-called “Green Deal” policy is the firm belief that the increase in CO_2 concentrations in the Earth’s atmosphere due to the burning of fossil fuels is the cause of the global warming threatening humanity. The number of publications in scientific journals seems to confirm this belief and make it an indisputable certainty. This takes advantage of the fact that CO_2 has absorption bands in the infrared range, as well as the results of geological studies showing a high correlation between changes in CO_2 concentration in the atmosphere and temperature changes over thousands of years [1]. This is taken as a solid scientific argument supporting this thesis.

Greenhouse gases, and CO_2 in particular, were brought to the attention of the prominent Swedish chemist and founder of physical chemistry, Svante Arrhenius, as early as the nineteenth century. He predicted that CO_2 produced by burning coal would cause our planet to warm [2]. However, just four years after Arrhenius’ publication, prominent Swedish geophysicist Knut Ångström showed that the absorption of the Earth’s thermal radiation in atmospheric carbon dioxide could not exceed 16% regardless of CO_2 concentration [3]. In recent years, many climatologists have tried to disprove this claim. With the help of theoretical analyses, qualitatively taking into account the broadening of the absorption lines of CO_2 at its high concentration, attempts are made to prove that the absorption spectrum of this gas will completely coincide with the spectrum of the Earth’s thermal radiation, and therefore this radiation can be entirely absorbed by CO_2. This hypothesis, which contradicts Ångström’s conclusions supported by the results of experimental work described in papers [4], [5], is used as a certainty in glazing models and in shaft models and general circulation models [6]–[8].

With this approach, the conclusions drawn from the so-called multi-window models lead, among other things, to the conclusion that with a sufficiently high concentration of CO_2 in the Earth’s atmosphere, the Earth’s temperature will be similar to that of Venus. Moreover, in general circulation models, in addition to the erroneous assumption of full coverage of the spectrum of radiative absorption in CO_2 with the thermal spectrum of the Earth at sufficiently high concentrations of this gas, uncertain input data are still assumed, since it is impossible to determine the exact initial and boundary conditions for the differential equations solved there, and any averaging with non-linear dependencies, must lead to serious errors. However, there are articles, including [10]–[21], which

show that most models do not take into account a number of important factors that can have a significant impact on the final result.

It is also worth noting that the accepted alleged evidence for the effect of increasing atmospheric CO_2 concentration on the increase in Earth's temperature is based on numerical experiments designed to confirm the veracity of the assumed climate models [22]. It is also worth noting that the evidence to date on the impact of CO_2 concentration in the atmosphere on its temperature is based on numerical experiments designed to confirm the validity of climate models [22]. There is a very clear lack of experimental work. This fact was pointed out in 2018 by the well-known and respected geophysicist Prof. Peter L. Ward (USA). In his speech (American Meteorological Society, 98th Annual Meeting 2018) [23] entitled "Climate sensitivity has never been demonstrated experimentally in the laboratory or in the field", he emphasizes that "Surprisingly, it has never been demonstrated experimentally that an increase in greenhouse gas concentrations causes the observed global warming".

The eminent climatologist John E. Harries expresses a similar view on this subject, stating in his work [24] that "The results presented here provide (to our knowledge) the first experimental observation of changes in the Earth's outgoing longwave radiation spectrum, and therefore the greenhouse effect: **previous studies have been largely limited to theoretical simulations because of the paucity of data**".

Experimental proof of a theory is the cornerstone of the scientific method. As Steven Chu put it [25]: "the ultimate arbiter of any point of view is experiments that seek impartial truth".

Given the facts presented above, it was necessary to plan an experiment in which the absorption of IR radiation by atmospheric CO_2 can be directly measured and justified on the basis of the laws of physics. Therefore, in the presented work, the authors on the ground of experimental facts analyze and draw conclusions about the interaction of thermal radiation with carbon dioxide in relation to the Earth's atmosphere and thermal radiation of the Earth.

2. Facts indicating carbon dioxide saturation of the Earth's thermal radiation absorption and radiative forcing under current conditions

It should be recalled that the term "saturation of absorption by carbon dioxide" means a state in which, as the mass of carbon dioxide absorbing radiation increases, the absorption of that radiation does not increase. Radiative forcing is the difference between the flux of thermal radiation energy from the Earth's surface through a hypothetical transparent atmosphere and the flux through an atmosphere containing greenhouse gases.

The IPCC reports [26], [27] and most articles on climate change present conclusions indicating that rising CO_2 concentrations in the atmosphere affect the climate and that there is no saturation of the Earth's heat radiation absorption by carbon dioxide. In contrast, the studies described in the following subsections present facts that contradict these conclusions.

2.1. Ångström–Koch experiment

It is a fact that a large part of the absorption spectrum of CO_2 overlaps with that of the Earth's thermal radiation, and therefore there must be absorption of this radiation and a weakening of its cooling capacity for our planet. But, as the eminent Swedish geophysicist Knut Ångström noted more than 120 years ago, with a sufficiently high concentration of CO_2 in the air, there is a saturation of the absorption of this radiation [3]. He drew these conclusions based on an analysis of the results of experimental work done in the laboratory by his assistant Koch, in which the transmission of thermal radiation in carbon dioxide was measured. These experiments showed, among other things, that in a layer 30 cm thick at a pressure of 780 Tr CO_2 there is a saturation effect of blackbody radiation absorption, because when this pressure is reduced to 2/3 of the initial value, the absorption changes slightly - by a maximum of 0.4 percent. On the basis of a closer analysis of the results of all the studies carried out by Koch, Ångström concluded that at most about 16 percent of the Earth's radiation is absorbed by atmospheric carbon dioxide regardless of the magnitude of the concentration of CO_2 in the air, and furthermore, with the

concentration of CO_2 in the atmosphere already existing at the time, changes in this concentration have very little effect on the total absorption of the Earth's thermal radiation. Ångström also referred to the well-known experiments of Svante Arrhenius [2], on the basis of which Arrhenius tried to justify that there is no saturation of the Earth's absorption of thermal radiation in atmospheric carbon dioxide. He noted that in these experiments the relatively large width of the spectrometer slit, which Arrhenius had to use so that with the relatively low sensitivity of the thermocouple used he could measure the intensity of the radiation used, did not allow an accurate check of the spectrum of lunar radiation. Therefore, the results of Arrhenius' further calculations must be viewed with serious skepticism, and no conclusions can be drawn from them regarding the impact of CO_2 in the atmosphere on the Earth's temperature. It should be clearly emphasized here that Ångström drew his conclusions based on an experiment in which, as in the experiments described later in this paper, all phenomena related to radiation absorption had to occur both at the center of the line and at the wings. The measurement results obtained by Ångström and in the experiments described in the paper were "final" results and therefore could not fail to take into account the broadening of the absorption lines. Furthermore, the frequent claims in discussions that Koch's tube was "too short" defy simple logic. If saturation is observed in a short tube, it will be even more pronounced in a longer tube.

2.2. Justification Dieter Schildknecht

Currently, the issue of the saturation of the Earth's thermal radiation absorption by atmospheric carbon dioxide has been convincingly explained by Dieter Schildknecht [28], among others. Based on numerical estimates of radiation transfer and using data from the HITRAN database, Schildknecht considered the argument put forward by Alfred Schack, who in 1972, based on experimental studies, claimed that there is saturation of Earth's infrared radiation absorption by atmospheric carbon dioxide when its concentration exceeds approximately 300 ppm [29]. In his work, Schack showed that for a concentration of 0.03% carbon dioxide in the air, saturation is reached at a distance close to the height of the troposphere. Therefore, further increases in the concentration of these gases cannot lead to a significant increase in radiation absorption and, consequently, cannot affect the Earth's temperature. Based on detailed data on CO_2 spectral absorption lines, Schildknecht, like Schack, assumed that the absorption of terrestrial thermal radiation in the atmosphere is determined by the mass of CO_2 per unit area perpendicular to the direction of propagation of the irradiated radiation. In his work, he determined the absorption coefficient and total absorption of thermal radiation in a mixture of CO_2 and air at a constant temperature and pressure in a hypothetical pipe from the Earth's surface to the end of the atmosphere. The results for individual sections of this pipe are presented in Table 2.1 and Fig. 2.1.

Table 2.1. Absorption of radiation from 600 to 750 cm^{-1}
for selected sections of pipe *l* from 1 to 7 km and concentrations *c* from 280 to 1000 ppm

l [km]/*c* [ppm]	280	300	380	400	600	760	1000
1	0.78	0.79	0.82	0.83	0.87	0.89	0.92
2	0.86	0.87	0.89	0.90	0.93	0.95	0.97
3	0.90	0.91	0.93	0.93	0.96	0.97	0.98
5	0.94	0.95	0.96	0.97	0.98	0.99	0.99
7	0.96	0.97	0.98	0.98	0.99	1.00	1.00

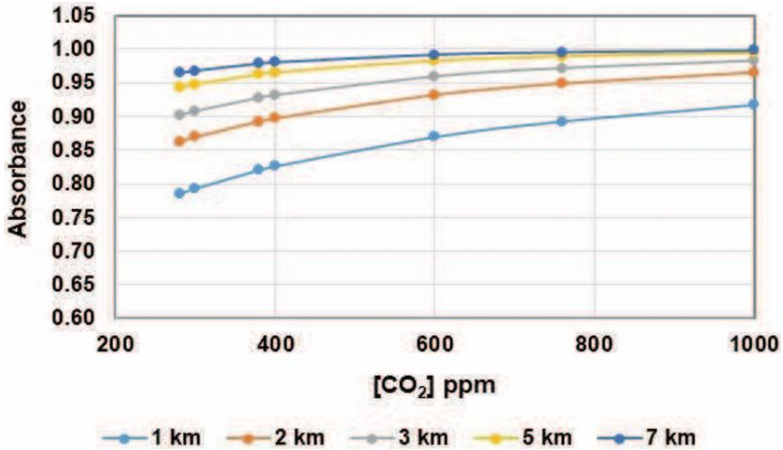

Fig. 2.1. Plots of the dependence of absorbance on CO_2 concentration
for selected sections of the pipe [28]

Next, Table 2.2 shows selected results of calculating absorption A and its percentage increase Δ and decrease in the power of the transmitted radiation, with an increase in CO_2 concentration from 300 to 600 ppm.

Table 2.2. Radiation absorption in CO_2 *A*, its percentage increase $\Delta_{2\times CO_2}$ [%]
and power decrease $\Delta_{2\times CO_2}$ [Wm^{-2}] for selected lengths
of pipe fragments *l* and CO_2 concentrations *c*

l [km]	*A* 300 ppm	*A* 600 ppm	$\Delta_{2\times CO_2}$ [%]	$\Delta_{2\times CO_2}$ [Wm^{-2}]
1	0.63	0.71	8	7.00
2	0.71	0.78	7	6.09
3	0.75	0.82	7	6.09
5	0.81	0.87	6	5.22
7	0.84	0.89	5	4.35

As a result of the calculations, the absorbance spectrum shown in Fig. 2.2 was obtained for a section of pipe 3 km long and for CO_2 concentrations of 0.03% and 0.06%.

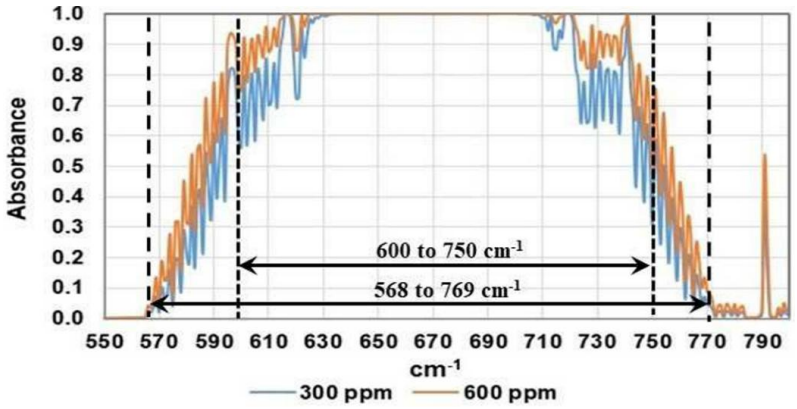

Fig. 2.2. Absorbance for CO_2-air mixture with concentrations of 0.03% and 0.06% for a section of pipe 3 km long and for CO_2 concentrations of 0.03% and 0.06% [28]

In the transition from a constant temperature T in a tube of CO_2 with air to a decreasing temperature T with altitude and a decreasing pressure p in the atmosphere, two stages were used. In the first stage, modeling a dry atmosphere, the effect of CO_2 (at concentrations of 0.03% and 0.06%) was considered, and in the second stage, water vapor was added at a constant relative humidity (RH) selected as RH = 85%. For the calculations performed, Table 2.3 gives the values of absorption A of thermal radiation of the Earth for the spectral range 568 cm^{-1}–769 cm^{-1}.

Table 2.3. Radiation absorption in CO_2 A and its percentage increase and decrease in radiant power with doubling of CO_2 concentration, for pipe sections of selected lengths

l [km]	A 300 ppm	A 600 ppm	$\Delta_{2\times CO_2}$ [%]	$\Delta_{2\times CO_2}$ [Wm^{-2}]
5 km	0.74	0.81	7	6.09
9 km	0.76	0.83	7	6.09
11 km	0.76	0.83	7	6.09

The results in Table 2.3 show that as the length of the pipe fragment increases, the absorption initially increases relatively quickly to reach a quasi-asymptotic limit for lengths just over 5 km. The assumed length of the pipe fragment corresponds to the corresponding height in the atmosphere. The calculated absorbance of thermal radiation

from the Earth's surface at 293 K for a dry atmosphere up to an altitude of 7 km, with CO_2 concentrations of 300 and 600 ppm, is shown in Fig. 2.3.

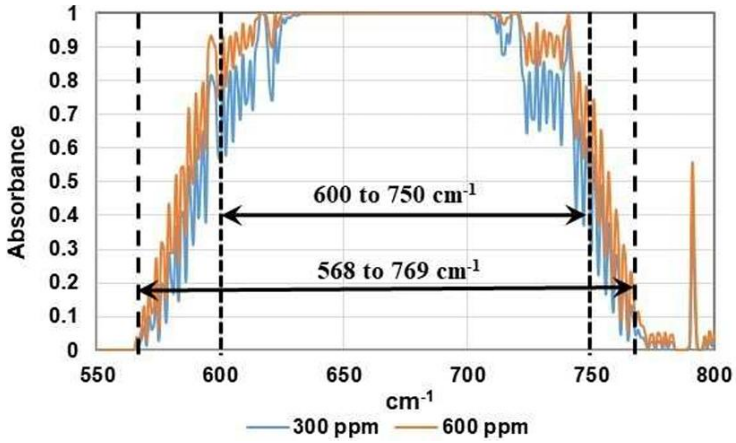

Fig. 2.3. Radiation absorption for a mixture of CO_2 and air with concentrations of 0.03% and 0.06% for a dry atmosphere in a section of vertical pipe from the Earth's surface to a height of 7 km [28]

The results show little effect of the doubling effect of CO_2 concentration in the atmosphere on the absorption of thermal radiation.

The paper also discusses the effect of water vapor on radiation absorption when doubling the CO_2 concentration. The results of calculations for the spectral range from 568 to 769 cm^{-1}, taking into account the absorption of radiation in water vapor at RH = 85%, are shown in Table 2.4.

Table 2.4. Absorption A of radiation from 568 to 769 cm^{-1} in CO_2 and its percentage increase ΔA [%] and decrease in radiant power ΔP [Wm^{-2}] for selected heights in the atmosphere and selected CO_2 concentrations taking into account absorption by water vapor at 85% relative humidity (RH)

l [km]	A 300 ppm	A 600 ppm	ΔA [%]	ΔP [Wm^{-2}]
5	0.89	0.92	3	2.6
9	0.90	0.93	3	2.6
11	0.90	0.93	3	2.6

The results for the spectrum from 600 to 750 cm^{-1} are shown in Table 2.5.

It can be seen that at RH = 85%, for both spectral ranges, the effect of CO_2 on the climate when its concentration is doubled, is drastically reduced. This is also shown in

the atmospheric absorption spectrum of radiation in the presence of water vapor shown in Fig. 2.4.

Table 2.5. Absorption A of radiation from 600 to 750 cm^{-1} in CO_2 and its percentage increase ΔA [%] and decrease in radiant power ΔP [Wm^{-2}] for selected heights in the atmosphere and selected CO_2 concentrations including absorption by water vapor at 85% relative humidity (RH)

l [km]	A 300 ppm	A 600 ppm	ΔA [%]	ΔP [Wm^{-2}]
5	0.94	0.97	3	2.0
9	0.95	0.98	3	2.0
11	0.95	0.98	3	2.0

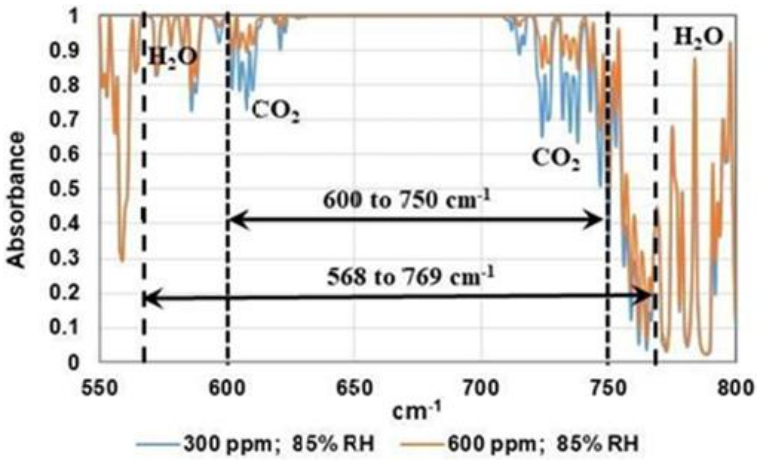

Fig. 2.4. Absorbance of thermal radiation for a mixture of CO_2 and air with concentrations of 0.03% and 0.06% in a humid atmosphere (85%) in a section of a vertical pipe from the Earth's surface to a height of 7 km [28]

Analyzing the phenomenon of the effect of absorption of thermal radiation of the Earth in atmospheric CO_2 in the presence of water vapor, on the increase in the temperature of our planet, the author calculates the value of the feedback coefficient f, commonly accepted in climatology, defined by the formula

$$f = 1 - \frac{\Delta T^{(0)}}{\Delta T^{(H)}} = 1 - \frac{\Delta^{(0)}_{2\times CO_2}}{\Delta^{(H)}_{2\times CO_2}}, \tag{2.1}$$

where:

$\Delta T^{(0)}$ – Earth's surface temperature change with doubling of CO_2 concentration in the absence of water vapor,

$\Delta T^{(H)}$ – change in temperature of Earth's surface with doubling of CO_2 concentration in the presence of water vapor,

$\Delta^{(0)}_{2\times CO_2}$ – decrease in radiative power emitted into space with doubling of CO_2 concentration in the absence of water vapor,

$\Delta^{(H)}_{2\times CO_2}$ – decrease in radiative power emitted into space with doubling of CO_2 concentration in the presence of water vapor.

From these calculations, it is clear that contrary to the widely accepted information, especially by the IPCC [26], [27], that the coupling is positive, obtained from the tables presented, the value of the coupling is

$$f = 1 - \frac{6.09}{2.6} = -1.34.$$

This coupling has a negative value, and thus the effect of carbon dioxide on temperature rise in the presence of water vapor is less than in its absence.

The paper presents the results of a "numerical experiment." They differ significantly from the results of "numerical experiments" presented in the papers used in IPCC reports and thus undermine their credibility. In such a case, the decisive argument should be the results of experimental work verifying the calculations at every possible stage.

2.3. Theoretical description of radiation transfer in the atmosphere according to H. Harde

In article [30], the issue of CO_2 impact on Earth's temperature was presented in a very cautious manner, with a comprehensive approach based on molecular fundamentals. In it, the author takes into account the fact that with the saturation of the absorption of the Earth's thermal radiation at its propagation in the atmosphere there is a broadening of the absorption lines of CO_2 and the influence of "weak" lines on the absorption of radiation increases, but at the same time does not suggest a full coverage of the absorption spectrum of CO_2 with the spectrum of the Earth's thermal radiation.

In the graphs made in the paper based on numerical calculations (Fig. 2.5), it is clear that the doubling of CO_2 concentration, despite the saturation of absorption, practically did not increase the share of radiation interacting with carbon dioxide in the total radiation emitted by the Earth's surface.

Ultimately, the author's careful calculations show that *"altogether only about 0.6%, corresponding to 2.4 W/m^2 of the total terrestrial radiation (391 W/m^2 at 288.15 K) or 0.8% with respect to the total back radiation of 312 W/m^2, can contribute to an*

additional global heating at doubled CO_2 concentration (380 ppm → 760 ppm). This result demonstrates why a further increase in the CO_2 concentration only gives marginal corrections in the radiation budget".

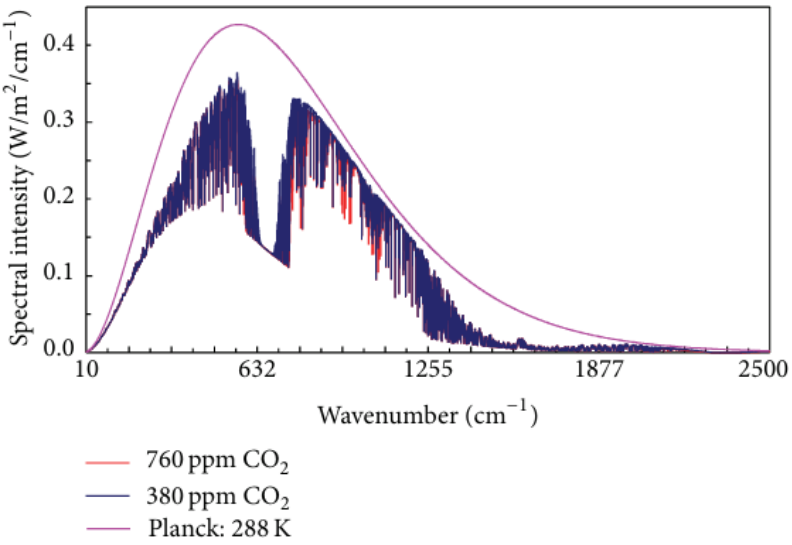

Fig. 2.5. Upwelling radiation at 12.5 km altitude with 380 ppm (blue line) and 760 ppm CO_2 (red line). Water vapour concentration is 14.615 ppm and temperature at ground 288 K [30]

The author validates the results obtained by comparing them with satellite measurements.

2.4. Satellite evidence of no significant impact of increased CO_2 concentrations in the atmosphere on the rise in its temperature

Article [24] analyzed the difference between the longwave radiation spectra emitted from Earth, as measured by orbiting spacecraft in 1970 and 1997. In the abstract, the authors state that their results "provide direct experimental evidence for a significant increase in the Earth's greenhouse effect", but whether this is really the case can be determined by analyzing these results again. The article analyzes the results of measurements taken on similar interferometers on satellites. The measurements were taken at intervals of almost three decades, with a relatively large increase in CO_2 concentration in the atmosphere. In 1970 (for a CO_2 concentration of 323.1 ppm) using the IRIS interferometric

spectrometer and in 1997 (for a CO_2 concentration of 363.467 ppm) using the IMG spectrometer[1]. The article describes the measurement method in detail and emphasizes the careful consideration of various factors affecting the results obtained. Ultimately, these results are illustrated in Fig. 2.6.

[1] Commonly used especially in radio astronomy and satellite remote sensing, brightness temperature is calculated based on the intensity of received electromagnetic radiation (e.g., microwave or infrared). It is expressed in Kelvins and corresponds to the temperature of a hypothetical black body, not necessarily the actual physical temperature of the object. There is a close relationship between brightness temperature and radiance [31], [32], expressed by the formula

$$I_v = B_v(T_b) = \frac{2hv^3}{c^2} \frac{1}{e^{\frac{hv}{kT_b}} - 1}.$$

This allows the radiation intensity I to be calculated from the considered spectral range Δv for which the brightness temperature distribution $T_b(v)$ is known.

The considerations presented in [24] cover a relatively wide spectrum of brightness temperatures and the impact of various greenhouse gases on them, but this paper only considers the impact of increased CO_2 concentrations on the rise in global temperatures. Therefore, wave number ranges where there is no absorption by CO_2 are not taken into account. Furthermore, wave number ranges where radiation absorption by CO_2 occurs but the brightness temperature does not change noticeably with increasing CO_2 concentration are also not taken into account. Thus, since careful analysis of the spectral results from both measurements by the authors of [24] did not reveal any differences in the brightness temperature spectrum for other wavenumber ranges corresponding to CO_2 absorption than in the range 710 cm^{-1}–780 cm^{-1}, it was decided that these ranges should not be taken into account, as they cannot have any impact on the final result.

Referring to the linearization of the brightness temperature spectrum function and the brightness temperature difference from the wave number (Figs. 2.7 and 2.8), it should be noted that, in practice, as a result of this approach, the value of both the observed brightness temperature and the brightness temperature difference was overestimated for almost the entire wave number range under consideration. Thus, the value of the reduction in radiation intensity ΔI from the considered frequency range has been overestimated, and in reality $\Delta I < 0.095$ $W \cdot m^{-2}$. Therefore, the actual increase in Earth's temperature caused by the increase in CO_2 concentration must be even smaller than the calculated 0.02°C.

It should also be noted that in real measurements, unlike in so-called "numerical experiments", the apparatus cannot ignore phenomena related to the broadening of absorption lines in CO_2 when radiation absorption is saturated.

Furthermore, satellite measurements record the final radiation emitted into space, regardless of whether it was emitted from warmer or colder layers.

Ultimately, therefore, the conclusions presented in this paper from the analysis of the results of [24] cannot raise any doubts as to their validity.

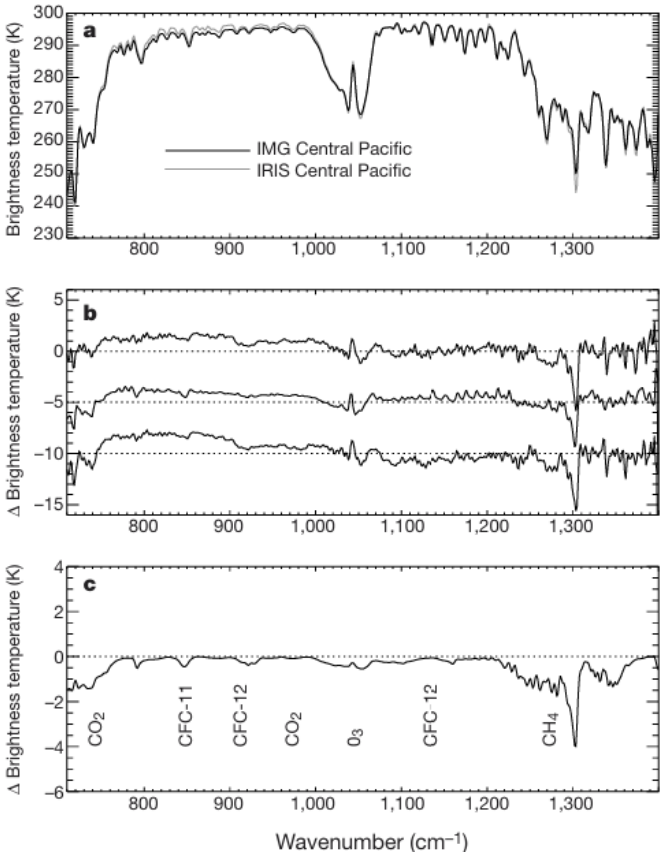

Fig. 2.6. Examples of observed and simulated IRIS and IMG spectra
for the three-month average (April–June) in selected regions [24]:
a) observed brightness temperature spectra under clear skies IRIS and IMG for the central Pacific,
b) top: observed differential spectrum taken from a); middle: simulated differential spectrum
for the central Pacific; bottom: observed differential spectrum for a larger area,
c) simulated spectrum component resulting solely from changes in trace gas concentrations.
The brightness temperature equivalent to the brightness temperature of a black body
is plotted on the ordinate axis

Figure 2.6a shows that the brightness of the atmosphere in the wavelength range corresponding to CO_2 absorption has changed so little that the difference is imperceptible. Only a more detailed analysis, resulting in the graph shown in Fig. 2.6c, shows that the brightness temperature for this wavelength range has decreased.

Therefore, it is necessary to check how this affects the increase in the Earth's surface temperature. Recall that the dependence of radiance on brightness temperature is expressed by the formula [31], [32]:

$$I(T_b) = \frac{2h}{c^2} \int_{\nu_1}^{\nu_2} \frac{\nu^3}{e^{\frac{h\nu}{kT_{b-1}}} - 1} d\nu, \tag{2.2}$$

where:

$h = 6.63 \cdot 10^{-34}$ J·s,

$k = 1.38 \cdot 10^{-23}$ J/K,

$c = 3 \cdot 10^{10}$ cm/s.

Moving from frequency ν to wave number $\tilde{\nu} \cdot (\nu = c\tilde{\nu})$, formula (2.2) can be written as

$$I(T_b) = 2hc^2 \int_{\tilde{\nu}_1}^{\tilde{\nu}_2} \frac{\tilde{\nu}^3}{e^{\frac{hc\tilde{\nu}}{kT_{b-1}}} - 1} d\tilde{\nu}. \tag{2.3}$$

To refer to the results presented in this paper, a section of Fig. 2.6 has been enlarged and presented in Fig. 2.7.

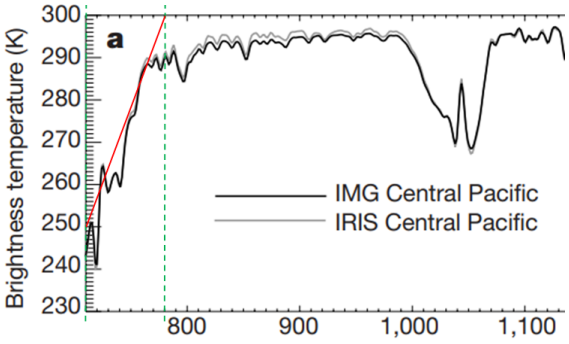

Fig. 2.7. Observed brightness temperature spectra under clear skies IRIS and IMG [24]

To determine the intensity of radiation emitted into space in the relevant wavelength range (710 cm^{-1}–780 cm^{-1}), Eq. (2.3) was used and the graph in Fig. 2.7 was parameterized for this wavelength range. It was assumed that changes in illumination temperature corresponding to the wavelength at which radiation is absorbed by CO_2 can be described by a linear function in the form:

$$T_b(\tilde{\nu}) = T_{b0} + a(\tilde{\nu} - \tilde{\nu}_0). \tag{2.4}$$

Referring to Fig. 2.7, the following assumptions were made:

$$T_{b0} = 250 \text{ K},$$

$$a = \frac{300\ \text{K} - 250\ \text{K}}{780\ \text{cm}^{-1} - 710\ \text{cm}^{-1}} = \frac{50\ \text{K}}{70\ \text{cm}^{-1}} \cong 0.7\ \text{K} \cdot \text{cm},$$

$$\tilde{\nu} = 710\ \text{cm}^{-1}.$$

After substitution into (2.4), a linearized dependence of brightness temperature on wave number in the range $\tilde{\nu} \in [710\ \text{cm}^{-1}, 780\ \text{cm}^{-1}]$ was obtained (red line).

$$\begin{gathered} T_b(\tilde{\nu}) = 250\ \text{K} + 0.7\ \text{Kcm} \cdot (\tilde{\nu} - 710\ \text{cm}^{-1}) = 0.7\ \text{Kcm} \cdot \tilde{\nu} - 247\ \text{K}, \\ T_b(\tilde{\nu}) = 0.7\ \text{Kcm} \cdot \tilde{\nu} - 247\ \text{K}. \end{gathered} \tag{2.5}$$

It can be assumed that this is the brightness temperature obtained from the first measurement.

After substituting into (2.3)

$$\begin{gathered} I(T_B) = 2hc^2 \int_{\tilde{\nu}_1}^{\tilde{\nu}_2} \frac{\tilde{\nu}^3}{e^{\frac{hc\tilde{\nu}}{k(0.7\ \text{Kcm} \cdot \tilde{\nu} - 247\ \text{K})}} - 1} d\tilde{\nu} \\ = 2 \cdot 6.63 \cdot 10^{-34}\ \text{J} \cdot \text{s} \cdot (3 \cdot 10^{10}\ \text{cm/s})^2 \int_{\tilde{\nu}_1}^{\tilde{\nu}_2} \frac{\tilde{\nu}^3}{e^{\frac{1.44\ \text{cm} \cdot \text{K} \cdot \tilde{\nu}}{0.7\ \text{Kcm} \cdot \tilde{\nu} - 247\ \text{K}}} - 1} d\tilde{\nu} \\ = 1.19 \cdot 10^{-12}\ \text{W} \cdot \text{cm}^2 \int_{\tilde{\nu}_1}^{\tilde{\nu}_2} \frac{\tilde{\nu}^3}{e^{\frac{1.44\ \text{cm} \cdot \text{K} \cdot \tilde{\nu}}{0.7\ \text{Kcm} \cdot \tilde{\nu} - 247\ \text{K}}} - 1} d\tilde{\nu}, \\ I(T_b) = 1.19 \cdot 10^{-12}\ \text{W} \cdot \text{cm}^2 \int_{\tilde{\nu}_1}^{\tilde{\nu}_2} \frac{\tilde{\nu}^3}{e^{\frac{1.44\ \text{cm} \cdot \text{K} \cdot \tilde{\nu}}{0.7\ \text{Kcm} \cdot \tilde{\nu} - 247\ \text{K}}} - 1} d\tilde{\nu}. \end{gathered} \tag{2.6}$$

After integrating the wave number range of interest: 710 $\text{cm}^{-1} \div 780\ \text{cm}^{-1}$, the intensity of radiation emitted into space from a unit area was obtained for the wave number range of radiation absorbed by CO_2 in the first measurement.

$$\begin{gathered} I(T_b) = 1.19 \cdot 10^{-12}\ \text{W} \cdot \text{cm}^2 \cdot 599\,030\,868\ \text{cm}^{-4} \\ = 7.12846733 \cdot 10^{-4} \frac{\text{W}}{\text{cm}^2} = 7.12846733 \frac{\text{W}}{\text{m}^2}, \\ I(T_b) = 7.12846733 \frac{\text{W}}{\text{m}^2}. \end{gathered} \tag{2.7}$$

A detailed analysis conducted by the authors of the study showed that between 1970 and 1997, the brightness temperature decreased by $\Delta T_b(\tilde{\nu})$ as a result of the increase in CO_2 concentration. This is shown in Fig. 2.8, which is an enlargement of Fig. 2.6c.

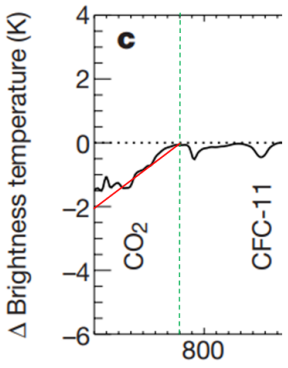

Fig. 2.8. Component of the simulated differential spectrum resulting solely from changes in CO_2 concentration [24]

As in the case of the graph in Fig. 2.7, the graph presented here has also been parameterized. It was assumed that changes in illumination temperature corresponding to the wave number for which radiation is absorbed by CO_2 can be described by a linear function in the form:

$$\Delta T_b(\tilde{\nu}) = -1.5\ \mathrm{K} + b(\tilde{\nu} - \tilde{\nu}_0). \tag{2.8}$$

Based on Fig. 2.8, the following values were:

$$b = \frac{0\ \mathrm{K} - (-2\ \mathrm{K})}{780\ \mathrm{cm}^{-1} - 710\ \mathrm{cm}^{-1}} = \frac{2\ \mathrm{K}}{70\ \mathrm{cm}^{-1}} = 0.0286\ \mathrm{Kcm} \approx 0.029\ \mathrm{Kcm},$$

$$\tilde{\nu} = 710\ \mathrm{cm}^{-1}.$$

After substitution into (2.8), a linearized dependence of the brightness temperature difference on the wave number in the range $\tilde{\nu} \in [710\ \mathrm{cm}^{-1}, 780\ \mathrm{cm}^{-1}]$ was obtained (red line in Fig. 2.8).

$$\begin{aligned} \Delta T_b(\tilde{\nu}) &= -2\ \mathrm{K} + 0.29\ \mathrm{Kcm} \cdot (\tilde{\nu} - 710\ \mathrm{cm}^{-1}) \\ &= -2\ \mathrm{K} + 0.029\ \mathrm{Kcm} \cdot \tilde{\nu} - 0.029\ \mathrm{Kcm} \cdot 710\ \mathrm{cm}^{-1} \\ &= 0.029\ \mathrm{Kcm} \cdot \tilde{\nu} - 22.6\ \mathrm{K}, \\ \Delta T_b(\tilde{\nu}) &= 0.029\ \mathrm{Kcm} \cdot \tilde{\nu} - 22.6\ \mathrm{K}. \end{aligned} \tag{2.9}$$

We can therefore express the new brightness temperature using the formula

$$T_{b1}(\tilde{\nu}) = T_b(\tilde{\nu}) + \Delta T_b(\tilde{\nu}).$$

After substituting (2.5) and (2.9), the following was obtained for the second measurement

$$\begin{aligned} T_{b1}(\tilde{\nu}) &= T_b(\tilde{\nu}) + \Delta T_b(\tilde{\nu}) \\ &= 0.7\ Kcm \cdot \tilde{\nu} - 247\ K + 0.029\ Kcm \cdot \tilde{\nu} - 22.6\ K \\ &= 0.729\ Kcm \cdot \tilde{\nu} - 269.6\ K, \\ T_{b1}(\tilde{\nu}) &= 0.729\ Kcm \cdot \tilde{\nu} - 269.6\ K. \end{aligned} \tag{2.10}$$

Proceeding in the same way as in the first measurement, we obtain

$$I(T_{b1}) = 1.19 \cdot 10^{-12}\ \mathrm{W \cdot cm^2} \int_{\tilde{\nu}_1}^{\tilde{\nu}_2} \frac{\tilde{\nu}^3}{e^{\frac{1.44\ \mathrm{cm \cdot K \cdot \tilde{\nu}}}{0.729\ \mathrm{Kcm \cdot \tilde{\nu} - 269.6\ K}}} - 1} d\tilde{\nu}. \tag{2.11}$$

After integration

$$\begin{aligned} I(T_b) &= 1.19 \cdot 10^{-12}\ \mathrm{W \cdot cm^2} \cdot 591\,024\,875\ \mathrm{cm^{-4}} \\ &= 7.03320 \cdot 10^{-4}\ \frac{\mathrm{W}}{\mathrm{cm^2}} = 7.03320\ \frac{\mathrm{W}}{\mathrm{m^2}}, \\ I(T_b) &= 7,03320\ W \cdot m^{-2}. \end{aligned}$$

The radiation intensity in the frequency range overlapping with the CO_2 absorption spectrum decreased by a value of

$$\Delta I = I(T_b) - I(T_{b1}) = 7.128\ \frac{\mathrm{W}}{\mathrm{m^2}} - 7.033\ \mathrm{W \cdot m^{-2}} = 0.095\ \mathrm{W \cdot m^{-2}}.$$

The intensity of thermal radiation emitted by the Earth's surface as a gray body can be determined using the formula

$$I_E = \varepsilon \cdot \sigma_B \cdot T_E^4, \tag{2.12}$$

where $\sigma_B = 5.67 \cdot 10^{-8}\ \mathrm{Wm^{-2}K^{-4}}$ – Stefan–Boltzmann constant.

Assuming an average temperature $T_E = 288$ K for the Earth's surface and an emissivity coefficient $\varepsilon = 0.85$ [33, 34], the intensity of radiation emitted by the Earth's surface should be

$$\begin{aligned} I_E &= \varepsilon \cdot \sigma_B \cdot T_E^4 = 0.85 \cdot 5.67 \cdot 10^{-8}\ \mathrm{Wm^{-2}K^{-4}} \cdot 288^4\ \mathrm{K^4} \cong 330\ \mathrm{Wm^{-2}}, \\ I_E &= 330\ \mathrm{Wm^{-2}}. \end{aligned}$$

As a result of the increase in carbon dioxide concentration in the atmosphere from 325 ppm in the first measurement to 364 ppm in the second measurement (by 12%), the intensity of radiation cooling the Earth decreased by $\Delta I = 0.095\ \mathrm{W \cdot m^{-2}}$.

To maintain energy balance, the Earth's temperature must increase by an amount ΔT_E such that

$$\begin{gathered} \varepsilon \cdot \sigma_B \cdot (T_E + \Delta T_E)^4 - \varepsilon \cdot \sigma_B \cdot T_E^4 = 0.095\ \mathrm{W \cdot m^{-2}}, \\ 0.85 \cdot 5.67 \cdot 10^{-8}\ \mathrm{Wm^{-2}K^{-4}} \cdot ((288\ \mathrm{K} + \Delta T_E)^4 - (288\ \mathrm{K})^4) = 0.095\ \mathrm{W \cdot m^{-2}}. \end{gathered} \tag{2.13}$$

Hence

$$\Delta T_E \approx 0.02\ \mathrm{K} = 0.02^{\circ}\mathrm{C}.$$

It follows that, contrary to the statements made in the introduction to the article, "Our results provide direct experimental evidence for a significant increase in the Earth's greenhouse effect", the analysis shows the opposite phenomenon.

The presented measurement results show that over a period of almost three decades, despite a 12% increase in CO_2 concentration in the atmosphere, the increase in Earth's temperature caused by this increase is only 0.02°C, which is practically negligible.

2.5. Experimental study of back radiation from CO_2

The authors of the paper [35] refer to many works in the introduction and state that the back radiation from the atmosphere directed downward shows full saturation for the IR band of CO_2. Therefore, there can be no noticeable additional thermal forcing (TF) by increasing the concentration of CO_2 in the atmosphere. It has been pointed out that the importance of unsaturated edges in the 15 μm band is commonly greatly exaggerated, since it can be easily shown that at a reduction <3 their contribution to the full band is only 0.17% when their respective integrals are considered. Cited, among others, are papers [28] and [29], whose results differ greatly from those officially accepted by the IPCC and other climate centers. In addition, based on the parameters used from the literature, the authors made the plots shown in Fig. 2.8 of the absorption of infrared radiation in the atmosphere as a function of CO_2 concentration for different path lengths completely confirming the hypothesis of saturation of the processes taking place.

These results inspired an experiment to verify the predicted effect of CO_2 on Earth's temperature through radiation feedback, which further warms the Earth's surface. The experiment was performed using a kit consisting of a chamber filled with a CO_2–nitrogen mixture and an infrared detector. This kit was used in two variants. In the laboratory variant, the chamber was capped with by from below with polyethylene film and underneath

it was a suitable disk cooled to –25°C. In the "field" variant, the disk was removed and the chamber was inverted by 180° and its window aimed at a cloudless sky. Based on the measurements and previous considerations, the authors estimated the value of back radiation from the atmosphere for a given length of the air column under ground conditions for the corresponding CO_2 concentrations and specified path lengths. The results are shown in Fig. 2.10.

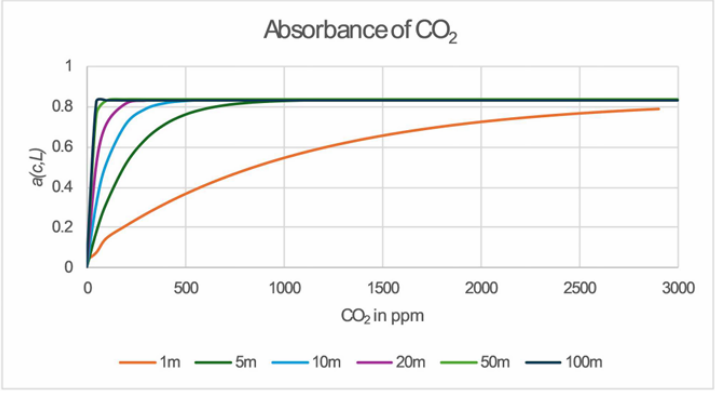

Fig. 2.9 Absorbance of infrared light as a function of CO_2 concentration for different path in the atmosphere [36]

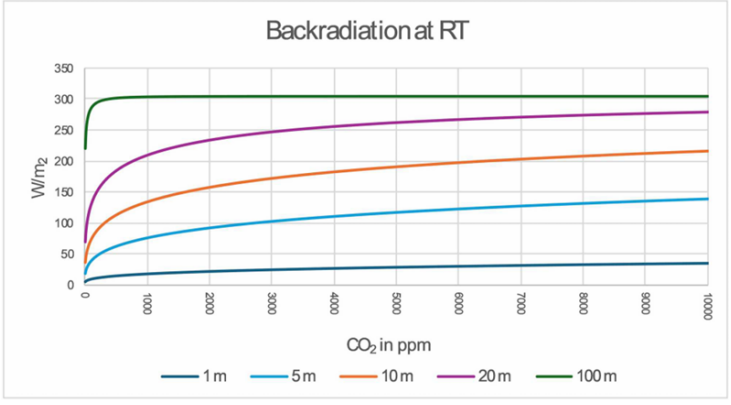

Fig. 2.10. Calculated back-radiation for different long air columns at room temperature (RT) [36]

Experimental evidence from this work supports the results of the work presented at the beginning, according to which increasing CO_2 concentrations in the atmosphere at current levels cannot significantly contribute to warming by increasing radiative forcing.

2.6. Experimental absorption characteristics of thermal radiation in CO_2

Experimentally saturated absorption of thermal radiation by carbon dioxide was confirmed in the work [5]. Starting with the narrower issue of propagation of monochromatic radiation through an absorbing medium, a simplified analysis of the phenomena studied was carried out at the beginning of the paper. Passing a collimated beam of monochromatic radiation through a solution of a substance absorbing this radiation, one obtains, according to Lambert–Beer's law, the intensity of this radiation described by the formula:

$$I = I_0 e^{-\alpha l c}, \tag{2.14}$$

where:

I_0 – irradiance entering the sample,
I – irradiance after passing through the sample,
α – absorption mass coefficient [$m^2\ kg^{-1}$],
l – layer thickness [m],
c – mass concentration [$kg\ m^{-3}$].

Disregarding scattering processes, absorption, defined as the ratio of the energy of absorbed radiation to the energy of incoming radiation at a specific time, can be described by the formula:

$$A = \frac{I_0 - I}{I_0} = 1 - e^{-\alpha \cdot l \cdot c}. \tag{2.15}$$

By introducing a new quantity called the absorbing mass per unit area defined as $m = l \cdot c$, Eq. (2.15) takes the form:

$$A = 1 - e^{-\alpha \cdot m}. \tag{2.16}$$

As the value of m increases, the absorption asymptotically tends to a value of 1, and for a large enough value we can consider that we have a saturation.

It should be noted that the absorbing substance not only absorbs radiation, but also emits it. For monochromatic radiation, resonant absorption occurs for a strictly defined wavelength (within the line width), while spontaneous emission is the result of all possible transitions and the wavelength corresponding to the absorbed radiation accounts for a small share of it, omitted from Lambert–Beer's description.

The situation is different for the absorption of thermal radiation. In this case, both absorption and emission occur for all possible transitions. In addition, in the case of low-temperature radiation sources, we are dealing with a relatively low intensity of radiation. Then the thermal radiation emitted by the absorbing gas cannot be neglected. The situation is further complicated by the fact that with a relatively large number of oscillation-

rotation lines and their overlap at higher extinction values, the normalized line shape function $g(v)$, which describes the frequency–dependent interaction of radiation with particles, becomes very complex. Therefore, let's try to perform the considerations again, using the well-known Schwarzschild equation used in [36], among others:

$$\frac{dI_\lambda}{d\tau} = -I_\lambda + B_\lambda(T), \tag{2.17}$$

where:

$d\tau = k_\lambda \rho ds$,

τ – optical thickness measured rectilinearly (with neglecting refraction in the atmosphere),

k_λ – absorption mass coefficient,

ρ – density of the absorption medium,

s – propagation path,

$B_\lambda(T)$ – Kirchhoff–Planck's function.

Taking into account that the optical thickness is proportional to the mass of the absorbing substance m, and assuming a constant temperature of the gas (neglecting, among other things, its heating by the absorbed radiation), after integrating by frequency and neglecting the fact of broadening of the oscillation–rotation lines for large values of the absorbing mass, Eq. (2.17) can be written in the form:

$$\frac{dI}{dm} = -\alpha I + E, \tag{2.18}$$

where: α, E – constant.

The solution of Eq. (2.18) is of the form:

$$I = \left(I_0 - \frac{E}{\alpha} \right) e^{-\alpha m} + \frac{E}{\alpha}. \tag{2.19}$$

Using formula (2.16), we can write:

$$A = \frac{I_0 - I}{I_0} = 1 - \left(1 - \frac{E}{\alpha I_0} \right) e^{-\kappa m} - \frac{E}{\alpha I_0} = \left(1 - \frac{E}{\alpha I_0} \right) - \left(1 - \frac{E}{\alpha I_0} \right) e^{-\alpha m}. \tag{2.20}$$

By introducing the designation,

$$1 - \frac{E}{\alpha I_0} \equiv \psi \tag{2.21}$$

formula (2.20) will take the form:

$$A = \psi(1 - e^{-\alpha m}). \tag{2.22}$$

It should be noted that at equilibrium, when there are no additional heat sources in the absorbing medium, the intensity of radiation from spontaneous emission cannot be greater than the intensity of absorbed radiation. Therefore, the coefficient ψ can take values in the range $0 \leq \psi \leq 1$.

Equation (2.22) describing the propagation of a continuous (thermal) radiation beam, assuming no wing widening at saturation of the central part of the line, is similar to Eq. (2.16) and shows that, analogous to monochromatic radiation, the absorption of thermal radiation must saturate, tending towards the value ψ for a sufficiently large value of the absorbing mass m.

The considerations made were verified experimentally. A diagram of the experiment described in this work is shown in Fig. 2.11.

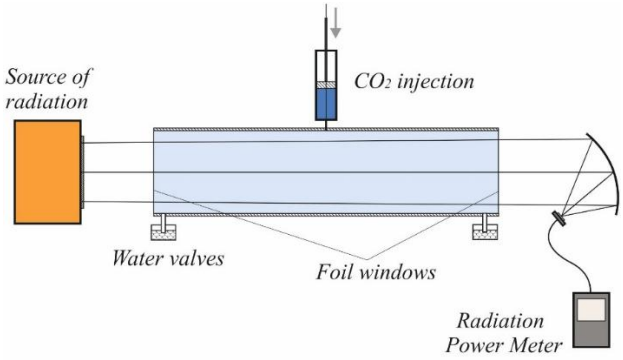

Fig. 2.11. Schematic of laboratory system
for measuring thermal radiation absorption in carbon dioxide

The experiment used a source of thermal radiation in the form of a glass vessel filled with mineral oil heated to a specific temperature, which, like the Earth's surface, was a source of continuous radiation.

It used a thermal radiation source in the form of a glass vessel filled with mineral oil heated to a certain temperature. A layer of graphite was applied to the flat side of this vessel, emitting the thermal radiation used. The absorption chamber was made in the form of a horizontal PVC pipe with a length of 1 m and a diameter of 150 mm, enclosed by polyethylene film windows. In the middle, a small, lockable hole was made in the cuvette for introducing a certain volume of carbon dioxide. At the ends of the cuvette, two hoses with tips immersed in water were brought out, constituting check valves through which a portion of the previous gas mixture, equal in volume to the volume of carbon dioxide injected, was ejected from the cuvette. The chamber was provided with mechanisms to ensure that the gases were mixed after each carbon dioxide injection.

Small portions of CO_2 were injected with a medical syringe, while a graduated vessel filled with carbon dioxide sealed at the bottom with a water jacket, which pushed the gas out through a tap at the top into the cuvette, was used to introduce larger portions. One hundred percent concentration of CO_2 in the cuvette was obtained by passing carbon dioxide from a cylinder through the cuvette over a 20-minute period and using a gas mixing device, and checking in the meantime whether absorption was increasing further.

The tests were conducted for two radiation source temperatures: 78.6°C and 109.5°C, reading the radiation power on the meter. Using Eq. (2.15) and taking I_0 as the radiation power for zero CO_2 concentration, the radiation absorption values were calculated from the readings. The results are recorded in Table 2.6.

Table 2.6. Absorption of thermal radiation in carbon dioxide

T = 78.6°C			T = 109.5°C		
No. measurement	m [kg/m^2]	A	No. measurement	m [kg/m^2]	A
1	0	0	1	0	0
2	0.00561	0.0177	2	0.00561	0.0031
3	0.01101	0.0402	3	0.01101	0.0171
4	0.02202	0.0524	4	0.02202	0.0303
5	0.03303	0.0595	5	0.03303	0.0454
6	0.06213	0.0749	6	0.06213	0.055
7	0.09081	0.0848	7	0.09081	0.0676
8	0.11907	0.0853	8	0.13548	0.0761
9	0.16311	0.1014	9	0.17912	0.0863
10	0.20613	0.1046	10	0.22192	0.0913
11	0.24831	0.1083	11	0.26369	0.0903
12	0.28945	0.1117	12	2.078	0.12
13	2.078	0.13			

Based on these, the graphs shown in Fig. 2.12 were made.

From the obtained graphs, it can be concluded that for the mass of carbon dioxide m_s = 1.5 kg/m^2, a state close to the saturation effect of A_s absorption was reached. For a source temperature of 78.6°C, the absorption of A_s = 0.13, while for a temperature of 109.5°C A_s = 0.12. From the obtained graphs it is also possible to read the values of the mass of CO_2, for which the value of absorption is equal to half the absorption of A_s. For a source temperature of 78.6°C $m_{1/2}$ = 0,049, while for 109.5°C $m_{1/2}$ = 0,078. By entering these values into Eq. (2.22), we can determine for a temperature of 78.6°C: ψ = 0.13, ψ_1 = 0.13, α_1 = 14.1 m^2/kg and for 109.5°C ψ_2 = 0.12, α_2 = 8.9 m^2/kg. After inserting

these values again into Eq. (2.22), graphs were obtained, which are shown as dashed lines in Fig. 2.13.

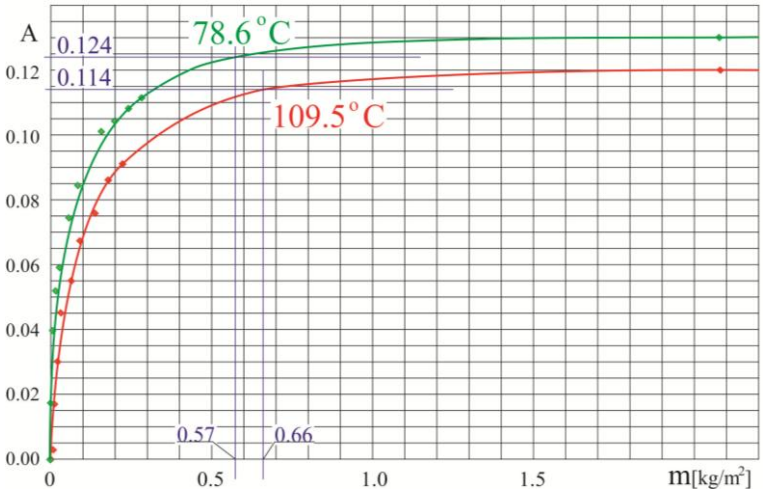

Fig. 2.12. Graph of absorption of thermal radiation as a function of absorbing mass of CO_2 for the source temperature of 78.6°C and 109.5°C, respectively

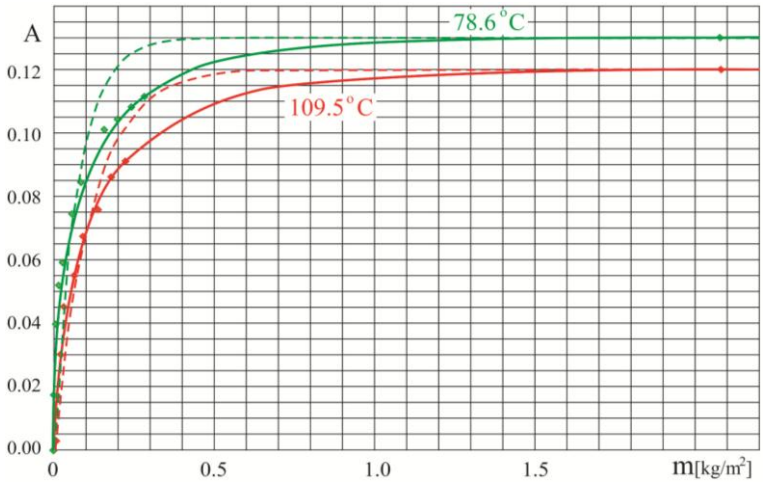

Fig. 2.13. Thermal radiation absorption graphs:
solid lines – experimental curves, dashed lines – curves made from Eq. (2.22)

The obtained graphs show that the actual saturation process is "slower" than the saturation process derived from formula (2.22). This is most likely due to the fact that

this formula does not take into account the complicated phenomenon of broadening of oscillation–rotation lines with an increase in the absorbing mass, which was mentioned at the beginning of the discussion. **It is therefore clear that widening the lines as a result of faster saturation of their central part than the wings only slightly slows down the entire process of radiation absorption saturation, but does not eliminate it.**

However, as can be seen, the saturation effect itself occurs and cannot be questioned. It should be noted that in the Earth's atmosphere, in a cylinder with a base area of 1 m^2 and a height from sea level to the stratosphere, there is a mass of carbon dioxide equal to:

$$m_{CO_2}\,[\text{kg}] = 1.52 \cdot 10^{-2}\ \text{kg} \cdot C_{CO_2}\,[\text{ppm}].$$

With a CO_2 concentration of 400 ppm, the value of the absorbing mass of carbon dioxide is about 6 kg/m^2. This mass is many times greater than the mass at which the saturation of thermal radiation absorption by carbon dioxide occurs.

This fact can be addressed critically. Carbon dioxide not only absorbs radiation but also emits it. This emission occurs in all directions. Thus, there is a component of it that coincides with the direction of radiation propagation from the Earth and thus amplifies this radiation.

This phenomenon will be discussed in detail in Chapter 4, while this chapter introduces the concept of effective transmission as the ratio of the final output radiation intensity to the radiation intensity entering the medium.

$$T_{ef} = \frac{I_0 - I_{abs} + I_{sp}}{I_0},$$

I_0 – intensity of input radiation,
I_{abs} – intensity of absorbed radiation,
I_{sp} – intensity of emitted radiation.

It should be noted that when there are large differences between the temperature of the radiation source and the temperature of the illuminated gas, spontaneous radiation is relatively small, and therefore effective absorption becomes "normal" absorption, as shown, among other things, in the formulas at the beginning of the subsection. For higher temperatures of the gaseous medium, spontaneous radiation begins to play an important role and "fills in the gaps" in absorbed radiation created by the absorption of this radiation in the gas. Ultimately, according to the second law of thermodynamics, the radiation flux can only decrease in value if the temperature of the illuminated gas is lower than that of the radiation source. In the experiment described here, for the case where the source temperature was 78.6°C (gas temperature 25°C), the temperature difference was 53.6 K. In order for the conditions of the experiment to correspond to real conditions, the

difference between the temperature of the radiator and the temperature of the absorbing gas should be similar for both cases.

Assuming an average temperature of the Earth's surface (radiant) of 15°C (288 K) and a temperature difference of 53.6 K, these conditions will be met for air with a temperature of 288 K –53.6 K = 234.4 K. According to Table 4.1, adopted in Chapter 4, in the atmosphere above 8.5 km, the temperature is lower than 233 K and thus is lower than 234.4 K and the pressure is 351 hPa. Therefore, from an altitude slightly lower than 8.5 km up to the stratosphere, the decrease in thermal radiative forcing as a function of CO_2 mass should be greater in the atmosphere than under experimental conditions. The mass of air with a temperature lower than 233 K in the vertical roller from 8.5 km to the stratosphere is:

$$m_{air}\left[\frac{\text{kg}}{\text{m}^2}\right]=\frac{p\,[\text{Pa}]}{g\left[\frac{\text{m}}{\text{s}^2}\right]}=\frac{35100\text{ Pa}}{9.8\frac{\text{m}}{\text{s}^2}}=3582\frac{\text{kg}}{\text{m}^2}.$$

In this air is dissolved carbon dioxide with a mass of

$$m_{\text{CO}_2}^{At}\left[\frac{\text{kg}}{\text{m}^2}\right]=\frac{M_{\text{CO}_2}}{M_{air}}\cdot m_{air}\left[\frac{\text{kg}}{\text{m}^2}\right]\cdot\frac{C_{\text{CO}_2}^{At}\,[\text{ppm}]}{10^6},$$

M_{CO_2} = 44 g – molar mass of CO_2, M_{air} = 29 – molar mass of air.

After substituting these values, for a CO_2 concentration of 400 ppm, the mass of carbon dioxide in the atmosphere that reduces thermal radiation is slightly greater than the mass $m_{\text{CO}_2}^{At}=2.178\frac{\text{kg}}{\text{m}^2}$. After plotting this value on the graph (Fig. 2.6), it can be seen that also after taking into account the second law of thermodynamics, at the current concentration of CO_2 in the atmosphere, we still have a complete saturation of the effective absorption of radiation emitted into space. With regard to the analysis carried out, it should be noted that the introduction of the concept of "effective absorption" does not ignore spontaneous radiation and thus takes into account so-called re-emission. The cuvette used in the experiment is incomparably shorter than the actual cylinder in the atmosphere, but when considering radiation absorption in gas, it is ultimately not the length of the path that matters, but the absorbance, and in the experiment conducted, by using a sufficiently high concentration of CO_2, this is comparable to real conditions. Furthermore, as already mentioned when discussing Ångström's experiment, if saturation occurs at lower absorbance, it will occur even more at higher absorbance. It should also be noted that water vapor and other gases whose absorption spectrum overlaps to any extent with that of CO_2 will reduce the intensity of radiation absorbed by this gas and thus cause absorption saturation to occur at a lower concentration. Ultimately, therefore, the experiment described shows that, contrary to the conclusions drawn from many

theoretical studies, despite the broadening of absorption lines, **the saturation of thermal radiation absorption in carbon dioxide dissolved in air is an indisputable fact.** The analysis also shows that in the Earth's atmosphere, at the current CO_2 concentration, this saturation should occur.

2.7. Moon experiment

Direct experimental confirmation that additional carbon dioxide in the atmosphere does not absorb thermal radiation from the Earth is provided by the lunar experiment described in the paper [4]. The illuminated lunar surface has a temperature of ~110°C. The moon reflects (scatters) only a little over 7% of sunlight. Therefore, infrared radiation from the illuminated lunar surface is practically thermal radiation emitted by the surface. Figure 2.14 shows the thermal radiation spectrum of the Moon, the thermal radiation spectrum of the Earth and the transmission spectrum of CO_2.

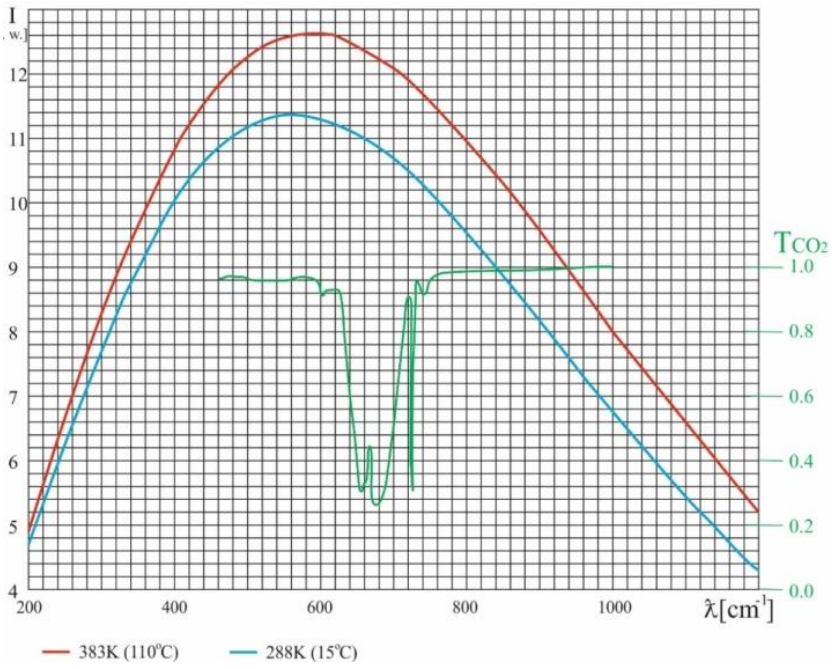

Fig. 2.14. The thermal radiation spectrum of the Moon (383 K),
the thermal radiation spectrum of the Earth (288 K) and the transmission spectrum of CO_2

The spectrum of both radiation near its maximum coincides with the absorption spectrum of CO_2 (HITRAN 2004). This makes it possible to use the Moon's thermal radiation to study the Earth's thermal radiation transmission.

The issue of using lunar radiation to study the Earth's atmosphere is not a new one. As already mentioned in Subsection 2.1, as early as the end of the nineteenth century, Professor Svante Arrhenius used it to study the absorption spectrum of gases in the atmosphere. What is new, however, is the approach itself. Without going into spectral details, a measurement of the Moon's thermal radiation transmission, after passing through the Earth's atmosphere, in additional carbon dioxide was now being made. Of course, the aforementioned details were taken into account in the design of the experiment, in the analysis of the measurement results and in the final conclusions drawn from the experiment.

Due to the partial overlap of the spectrum of the Moon's thermal radiation with the absorption spectrum of CO_2, the spectrum of such radiation when propagating through the Earth's atmosphere containing carbon dioxide should change. Thus, one should expect the formation of certain "holes" in the spectrum of the Moon's thermal radiation after passing through the Earth's atmosphere and thus reducing the absorption process of such radiation when propagating in additional carbon dioxide. To test this hypothesis, an experiment was performed, which consisted of two parts. The schematic of the system for the first part of the experiment is shown in Fig. 2.15.

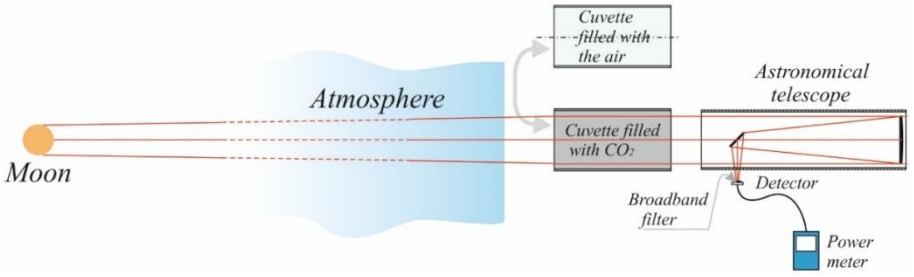

Fig. 2.15. Schematic of experimental setup for measuring infrared transmission from the Moon in supplemental carbon dioxide

The system used two identical cuvettes in the form of Plexiglas tubes with a diameter of 250 mm and a length of 500 mm closed with polyethylene film windows. One cuvette was filled with carbon dioxide, while the other, used as a reference cuvette, was filled with air. Radiation from the Moon, after passing through the cuvette, was focused by a Soligor MT-800/8 "E astronomical telescope on the S401C head of the PM200 power meter from THORLABS. The active surface of the measurement head was obscured by a broadband filter in the form of a flat-parallel germanium plate with the transmission spectrum shown in Fig. 2.16.

The experiment was conducted on a cloudless December night during the full moon at ~4°C on the terrace of a building in Warsaw. With the system oriented toward

a clear sky (away from the moon's disk), the power meter was zeroed and then, after pointing the optical axis to the center of the moon's disk, the power of the radiation incident on the meter head was measured. Alternately, the power of radiation from the moon was measured after passing through an absorption cuvette filled with carbon dioxide and through the same reference cuvette filled with air without CO_2. At the time of the measurement, the axis of the optical system of the cuvette and telescope pointing to the center of the Moon was deviated from the vertical by an angle of ~35°. Based on 50 readings taken every 0.01 s, the radiant power was determined. For ten consecutive measurements taken within five seconds each, the results and their average values shown in Table 2.7 were obtained.

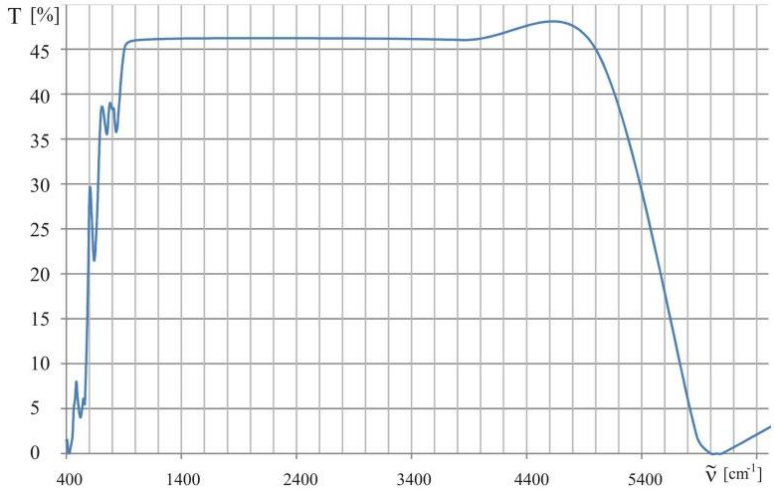

Fig. 2.16. Transmission spectrum of the germanium plate obscuring the measurement head

A view of the test stand is shown in Fig. 2.17.

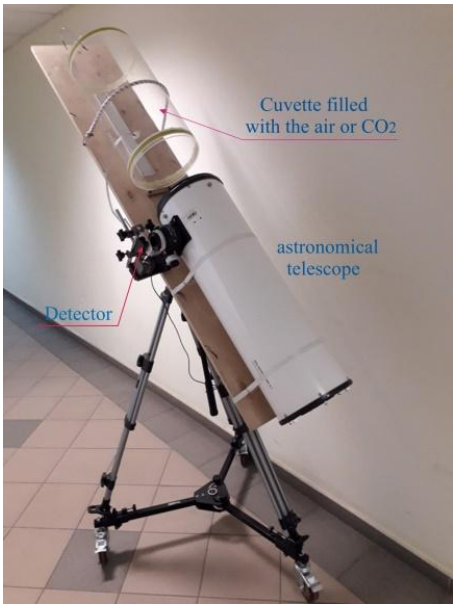

Fig. 2.17. View of the test stand for measuring infrared transmission from the Moon in carbon dioxide

Table 2.7. Power of infrared radiation from the Moon after passing through the corresponding cuvette

Setting	Radiation power for CO_2 cuvette [μW]	Setting	Radiation power for air cuvette [μW]
1	123.2	2	122.4
	121.7		123.1
	119.5		120.0
3	120.7	4	119.4
	122.1		121.3
	119.5		122.0
5	121.5	6	120.8
	119.1		118.3
	120.7		122.1
Average power	**120.9**	Average power	**121.0**

The second part of the experiment was carried out in the laboratory in a closed room according to the scheme shown in Fig. 2.18.

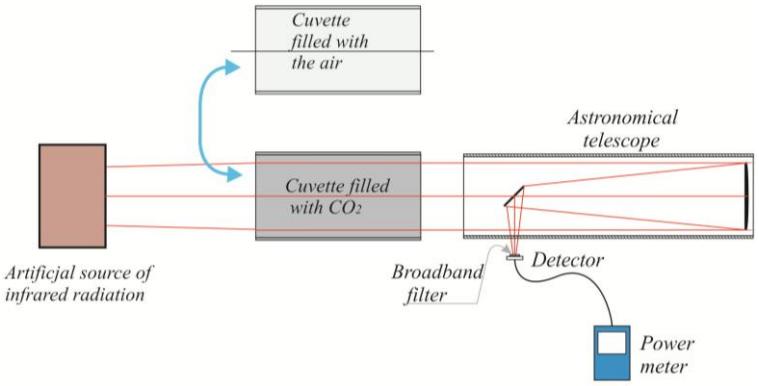

Fig. 2.18. Experimental setup for measuring infrared transmission through a CO_2 cuvette

It used the setup described in the first part of the experiment, replacing the Moon with a reference radiation source. This source consisted of a 100 mm diameter and 150 mm high circular glass vessel filled with mineral oil. The vessel was thermally insulated with polyurethane foam with a 40 mm diameter hole for the emitted radiation. The emitting surface of the vessel (behind the hole in the foam) was matted. Using an electric heater immersed in the oil, the oil was heated to 110°C. The emission surface of the radiation source was at a distance of 50 cm from the polyethylene window of the screened cuvette. Similarly to the first part of the experiment, the power of infrared radiation incident on the head of the radiation power meter was measured for the carbon dioxide cuvette and the air cuvette. The results of the measurements are shown in Table 2.8.

Table 2.8. The power of infrared radiation from the reference source after passing through the corresponding cuvette

Setting	Radiation power for CO_2 cuvette [µW]	Setting	Radiation power for air cuvette [µW]
1	267.2	2	310.4
	265.1		309.4
	263.7		308.5
3	264.6	4	309.2
	263.2		310.1
	262.9		308.9
5	264.2	6	307.9
	266.7		310.1
	263.9		308.7
Average power	**264.6**	Average power	**309.2**

It can be clearly seen that the thermal radiation from the simulator, not passing through the Earth's atmosphere, when passing through the CO_2 cuvette, experiences a weakening equal to the

$$A = \frac{309.2\ \mu W - 264.6\ \mu W}{309.2\ \mu W} \cong 0.14.$$

The conclusion of the lunar experiment

Infrared radiation from the Moon, after passing through the Earth's atmosphere, is not absorbed in carbon dioxide. The length of the cuvette was sufficient to show that the same radiation from the moon simulator, but not passing through the atmosphere, undergoes a significant attenuation in the same cuvette. The absorption process of infrared radiation with a continuous spectrum containing a band that overlaps with the absorption band of CO_2, regardless of whether the radiation comes from Earth or the Moon, is the same. It does not depend on the direction of propagation and the minimal shift of the spectrum related to temperature, cannot have a significant effect on it. Thus, thermal radiation from the Earth just like radiation from the Moon, after passing through the Earth's atmosphere, cannot be absorbed in additional carbon dioxide. This clearly shows that in the existing carbon dioxide in the atmosphere, all the absorbable radiation has been absorbed and the remaining radiation has a spectrum that does not overlap with the absorption spectrum of CO_2. Thus, for this radiation, additional carbon dioxide, like nitrogen and oxygen, is an inactive gas, unable to affect the temperature increase of the atmosphere in any way.

2.8. Comparison of periodic changes in global atmospheric CO_2 concentration with periodic changes in global temperature

An example that challenges the dogma that CO_2 is responsible for the Earth's temperature rise is the work of Norwegian professors: Ole Humlum, Kjell Stordahl and Jan-Erik Solheim in 2013 [37]. The authors, relying on data from a number of global databases containing measurements of temperature and atmospheric CO_2 concentration, presented graphs of these changes (Fig. 2.19). The values shown for global atmospheric CO_2 concentration and global sea surface temperature and global near-surface air temperature are for individual months in the period from 1982 to 2012. (Usually such averages are calculated for years or even whole decades.)

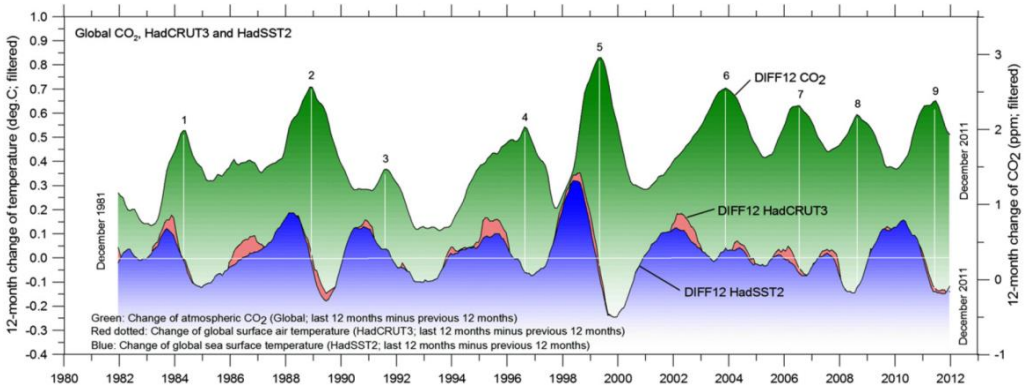

Fig. 2.19. Periodic change in global atmospheric CO_2 concentration (green), global sea surface temperature (blue) and global air temperature near the surface (red) [37]

The result of their work is surprising. It turns out that over the period studied, temperature changes precede changes in CO_2 concentration by several months. The question arises: if temperature changes are caused by changes in CO_2 concentration, why does the effect precede the cause?

The material developed proves that due to the saturation of the Earth's absorption of thermal radiation, additional carbon dioxide entering the atmosphere does not increase its temperature, but conversely, as a result of the increase in the Earth's temperature, carbon dioxide is most likely released from the oceans, causing an increase in its concentration in the atmosphere. This fact cannot be observed when we study the phenomenon over long periods of time, such as hundreds or thousands of years. Therefore, conclusions drawn from the results of glacier drilling and the results of sedimentary rock studies should be approached very cautiously.

3. Single-layer model of the atmosphere

The facts presented in Chapter 2 concerning the impact of CO_2 concentration in the Earth's atmosphere on its temperature inspire a vivid representation of the issue under consideration. Without going into detail, they can be presented in a simplified manner, as shown in Fig. 3.1.

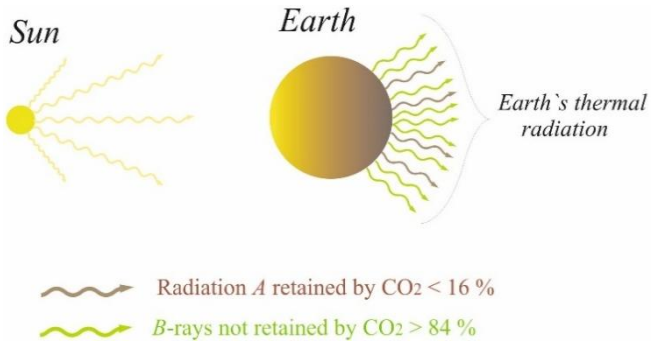

Fig. 3.1. Schematic drawing showing Earth's basic radiation processes

A stream of solar energy "reaches" our planet and warms it. At the same time, a stream of heat from the heated Earth "drains" into space and cools it. There is an equilibrium in which the Earth has a certain temperature. Of course, the stream of energy from the sun to the Earth is solar radiation, and the outflow stream is infrared radiation. As experimentally demonstrated 125 years ago by the aforementioned prominent Swedish geophysicist Knut Ångström [3], and now confirmed by experiments described in papers [4], [5], and also confirmed by available satellite images, the infrared radiation emitted by the Earth can be divided into *A* radiation, which is absorbed by carbon dioxide, and *B* radiation, which is not absorbed by this gas. The share of *A*-radiation in total infrared radiation is only a dozen or so percent. Carbon dioxide introduced into the atmosphere can only absorb *A*-radiation. Therefore, at a sufficiently high concentration of this gas, *A*-radiation is completely absorbed and a further increase in this concentration in the atmosphere is of no importance because for the remaining *B*-radiation it is an "inert" gas just like nitrogen and oxygen. Laboratory experiments and atmospheric

measurement data presented in Chapter 2 suggest that radiation A has already been completely absorbed at the existing concentration of CO_2 in the atmosphere.

A more precise description of this issue boils down to a discussion of the well-known Schwarzschild equation containing a term responsible for the absorption of the passing radiation and a term describing the spontaneous emission of excited atoms or molecules.

A more precise description of this issue boils down to a discussion of the well-known Schwarzschild equation containing the member responsible for absorption It should be noted that the Einstein spontaneous emission coefficient responsible for the emission of spontaneous radiation from molecules is inversely proportional to the third power of the wavelength. Thus, for the considered thermal radiation absorbed by atmospheric carbon dioxide, it is very small, since we are dealing with radiation of relatively long wavelength (~15μm). According to reliable literature data [38], the average "lifetime" of a CO_2 molecule that has absorbed a quantum of radiation with a wavelength of ~15μm is about one second. During this time, this molecule will experience billions of collisions with N_2 and O_2 molecules, exchanging its energy with them. Therefore, when considering the propagation of the Earth's thermal radiation in an atmosphere containing carbon dioxide, without ignoring the spontaneous radiation, we need not consider it together with the absorbed radiation emitted by the lithosphere.

Thus, assuming the aforementioned division of radiation and separating the absorption of this radiation from spontaneous emission, and assuming the absence of CO_2 in the atmosphere, the process of energy exchange on Earth can be illustrated using a single-layer model of the atmosphere according to the energy diagram shown in Fig. 3.2.

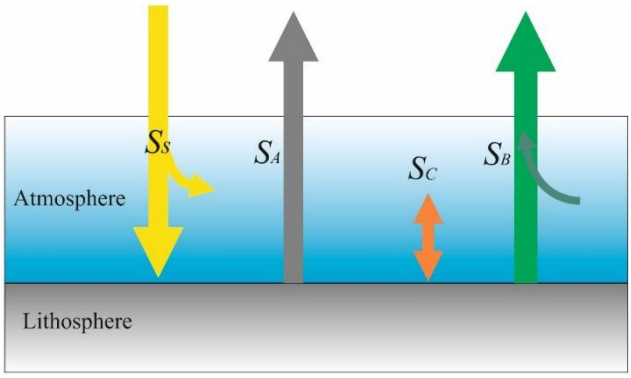

Fig. 3.2. Diagram of the energy transfer on Earth assuming no CO_2 in the atmosphere

It shows a stabilized state in which a certain temperature of the lithosphere and atmosphere is established as a result of the inflow of the solar energy flux S_S into the lithosphere and atmosphere and the outflow of the two energy fluxes S_A and S_B into space.

In the absence of CO_2 in the atmosphere, the S_A flux is A radiation reduced by absorption in vapors and gases with absorption spectra partially overlapping with that of CO_2. In contrast, the S_B flux is B radiation emitted from the lithosphere (hydrosphere) with a spectrum that does not overlap with the absorption spectrum of CO_2, also reduced by absorption in atmospheric vapors and gases, and spontaneous radiation leaving the atmosphere emitted by all gases in the atmosphere also with a spectrum that does not overlap with the absorption spectrum of CO_2.

S_C flux in the form of any energy exchange (not only radiative) between the lithosphere and the atmosphere should also be included in the considerations. It is the resultant of all factors that equalize the distribution of energy in the lithosphere (hydrosphere) – atmosphere system according to the laws of thermodynamics. It includes convection, thermal conduction, radiation and other factors. However, it should be clearly emphasized that this flux, when treating the lithosphere and atmosphere as a single object, is an internal factor that cannot affect the energy state of the whole. It should also be noted that both the S_A flux and the S_B flux, have their limited value depending only on temperature.

When a small amount of CO_2 is introduced into the atmosphere, there will be some changes shown in Fig. 3.3. Part of the S_A flux, marked as S'_A, will be absorbed by atmospheric carbon dioxide, causing the S_A flux to decrease and the atmosphere to heat up.

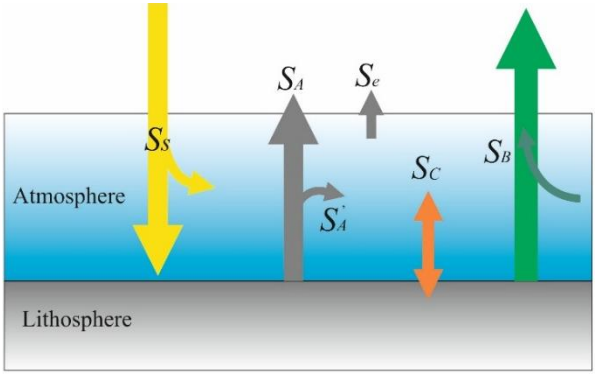

Fig. 3.3. Schematic of the energy transfer on Earth
for a small amount of CO_2 in the atmosphere

Through the S_C flux, the temperature of the lithosphere will also increase, causing a slight increase in the S_B flux and reducing the aforementioned decrease in the S_A flux. At the same time, carbon dioxide introduced into the atmosphere will emit spontaneous radiation in all directions. Horizontal fluxes, as a result of multiple absorption, will not affect the energy state of the atmosphere, the downward vertical flux will merge with the S_C flux, leading to an increase in the temperature of the lithosphere, while the upward vertical flux S_e (also reduced by absorption in the atmosphere), will discharge some energy into space.

However, once a large enough portion of CO_2 is introduced into the atmosphere, the entire S_A flux will be, in the form of S'_A flux, absorbed in the atmosphere (Fig. 3.4).

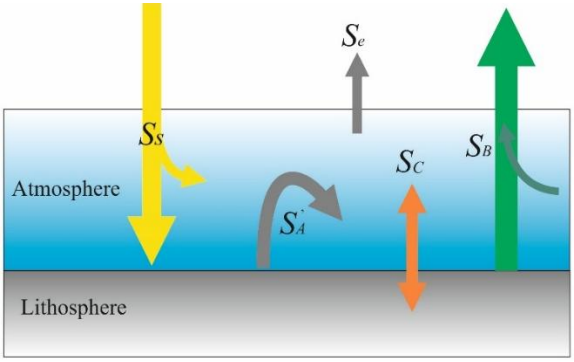

Fig. 3.4. Schematic of the energy transfer on Earth once the "saturation mass" of CO_2 in the atmosphere is exceeded

Increased atmospheric temperature and direct spontaneous emission from additional CO_2 molecules will increase the S_C and S_e fluxes. However, given that only a small fraction of the energy supplied to the atmosphere by the S_A´ flux passes to the S_e flux, the temperature of the atmosphere–lithosphere system should increase. However, as already mentioned, the value of the S_A flux that has completely passed into the S'_A flux is limited, determined by Boltzmann's law and the absorption spectrum. Therefore, once the S_A flux has fully passed into the S'_A flux (after CO_2 has completely absorbed *A*-radiation in the atmosphere), additional carbon dioxide cannot increase the energy input to the atmosphere because this energy will already be missing.

On the other hand, the S_e flux associated with atmospheric carbon dioxide must be zero in the absence of this gas and thus should be an increasing function of its concentration.

The hypothesis presented in many studies [39, 40], that with an increase in CO_2 concentration, spontaneous emission occurs in the higher, colder layer, and thus the Se flux must decrease with an increase in CO_2 concentration, ultimately leading to a significant reduction in the planet's cooling process, is false. The increase in this concentration does not reduce the dominant S_B stream in the slightest, and moreover, there is low pressure in the upper layers, and therefore the absorption lines, like the lines of the emitted radiation spectrum, narrow with altitude, broadening the spectrum of non-absorbable radiation. Therefore, additional carbon dioxide, once it exceeds a certain concentration – the "saturation state" – cannot reduce the outflow of energy into space.

Thus, **the arguments presented in Chapter 2 concerning the saturation of Earth's thermal radiation absorption at the current concentration of CO_2 in the atmosphere clearly show that further increases in this concentration do not contribute to an increase in the temperature of the Earth's atmosphere**.

4. The eight-layer model of the atmosphere

The width of the absorption line depends on the pressure and temperature of the absorbing gas. Therefore, it is necessary to repeat the experiment presented in Subsection 2.6 with the possibility of creating conditions in the laboratory such that the width of the absorption line of the CO_2 used is similar to the width of the line in the atmosphere at different altitudes. Therefore, this chapter analyzes the eight-layer model of the atmosphere and describes the experiment whose results were used as *input* data for this model.

4.1. Assumptions for the model

Absorption and spontaneous emission of radiation in a gas depend on the pressure and temperature of the gas. This is related, among other things, to the width of the oscillation–rotation lines, which is a function of pressure and temperature. Thus, these phenomena depend on the height in the troposphere. In order to account for this dependence, an eight-layer model of the troposphere was considered, the boundaries of which are at

Table 4.1. Parameters of the troposphere layers

Layer no.	Upper layer limit [km]	Temp. at end of layer [K]	Average temp. in the layer [K]	Pressure at the end of the layer [hPa]	Average layer pressure [hPa]
0	0.5	285	287	955	984
1	2.5	272	278.5	744	850
2	4.5	259	265.5	578	661
3	6.5	246	252.5	452	515
4	8.5	233	239.5	351	402
5	10.5	220	226.5	271	311
6	12.5	207	213.5	208	240
7	14.5	194	200.5	160	184

heights of, respectively: 500 m, 2500 m, 4500 m, 6500 m, 8500 m, 10 500 m, 12 500 m, 14 500 m. Based on the commonly known parameters recorded in the report [41], among others, the troposphere data shown in Table 4.1 were adopted.

The mass of air per unit horizontal area (perpendicular to the direction of radiation propagation) in the considered layer of the troposphere can be determined from the formula

$$m_{air}\left[\frac{\text{kg}}{\text{m}^2}\right]=\frac{\Delta p\,[\text{Pa}]}{g\left[\frac{\text{m}}{\text{s}^2}\right]}, \tag{4.1}$$

where Δp – pressure difference at layer boundaries, g = 9.8 m/s^2 – ground acceleration.

The mass of carbon dioxide per unit area perpendicular to the direction of radiation propagation in the considered troposphere layer for the concentration $c_{\text{CO}_2}^{At}$, is:

$$\begin{aligned} m_{\text{CO}_2}^{At}\left[\frac{\text{kg}}{\text{m}^2}\right] &= \frac{M_{\text{CO}_2}}{M_{air}}\cdot m_{air}\left[\frac{\text{kg}}{\text{m}^2}\right]\cdot\frac{C_{\text{CO}_2}^{At}\,[\text{ppm}]}{10^6} \\ &= \frac{44}{29\cdot 10^6}\cdot m_{air}\left[\frac{\text{kg}}{\text{m}^2}\right]\cdot C_{\text{CO}_2}^{At}\,[\text{ppm}] \\ &= 1.52\cdot 10^{-6}\cdot m_{air}\left[\frac{\text{kg}}{\text{m}^2}\right]\cdot C_{\text{CO}_2}^{At}\,[\text{ppm}], \end{aligned} \tag{4.2}$$

where M_{CO_2} = 44 – molar mass of CO_2, M_{air} = 29 – molar mass of air; $C_{\text{CO}_2}^{At}$ [ppm] – concentration of carbon dioxide in the atmosphere.

The conditions present in the different layers of the troposphere can be provided in the laboratory, using a suitable cuvette with windows that transmit the thermal radiation used. However, for the laboratory model to be adequate for real conditions, the mass of carbon dioxide per unit area perpendicular to the direction of the radiation beam must be the same in the cuvette as in the corresponding layer. This was ensured by selecting the appropriate partial pressure of CO_2. In addition, the total pressure and temperature in the cuvette must be such that the width of the oscillation-rotation lines is the same as in the layer under consideration.

In order to determine the necessary partial pressure of CO_2 in the cuvette, the following considerations were made. The equation of gas state for CO_2 in the cuvette can be written in the form:

$$\frac{p_{\text{CO}_2}^{K}\cdot V_K}{T_K}=n_{\text{CO}_2}\cdot R, \tag{4.3}$$

where:

$p^K_{CO_2}$ – partial pressure of CO_2 in the cuvette,

$V_K = S_{kw} \cdot l_K$ – the volume of the cuvette,

S_{kw} – the cross-sectional area of the cuvette,

$l_K = 0.96$ m – the length of the prepared cuvette,

T_K – the temperature of the gas mixture in the cuvette,

$n_{CO_2} = \dfrac{m^K_{CO_2}}{M_{CO_2}}$ – number of moles of CO_2 in cuvette,

$m^K_{CO_2}$ – mass of CO_2 in cuvette,

$M_{CO_2} = 44$ g – molar mass of CO_2,

$R = 8.31 \dfrac{\text{kg} \cdot \text{m}^2}{\text{K} \cdot \text{s}^2}$ – gas constant.

After transforming (4.3), we get:

$$p^K_{CO_2}\,[\text{Pa}] = 22.7 \frac{1}{\text{kg}} \cdot m^K_{CO_2}\,[\text{kg}] \cdot T_K \cdot \frac{8.31 \dfrac{\text{kg} \cdot \text{m}^2}{\text{K} \cdot \text{s}^2}}{S_{kw} \cdot l_K}. \tag{4.4}$$

The mass of CO_2 in the cuvette per unit transverse area of the cuvette must be the same as the mass of CO_2 per unit area in the atmosphere in the layer under consideration.

$$\frac{m^K_{CO_2}\,[\text{kg}]}{S_{kw}\,[\text{m}^2]} = m^{At}_{CO_2} \left[\frac{\text{kg}}{\text{m}^2}\right].$$

After taking into account equality (4.2), the following is obtained

$$\frac{m^K_{CO_2}\,[\text{kg}]}{S_{kw}\,[\text{m}^2]} = m^{At}_{CO_2} \left[\frac{\text{kg}}{\text{m}^2}\right] = 1.52 \cdot 10^{-6} \cdot m_{air}\,[\text{kg/m}^2] \cdot c^{At}_{CO_2}\,[\text{ppm}].$$

After substitution into (4.4), the required pressure of CO_2 in the cuvette can be described by the formula:

$$p^K_{CO_2}\,[\text{Pa}] = 2.987 \cdot 10^{-4} \cdot m_{air} \left[\frac{\text{kg}}{\text{m}^2}\right] \cdot c^{At}_{CO_2}\,[\text{ppm}] \cdot T_K\,[\text{K}]. \tag{4.5}$$

For the temperature in the cuvette $T_K = 298$ K (25°C)

$$p^K_{CO_2}\,[\text{Pa}] = 0.089 \frac{\text{m}}{\text{s}^2} \cdot m_{air} \left[\frac{\text{kg}}{\text{m}^2}\right] \cdot c^{At}_{CO_2}\,[\text{ppm}]. \tag{4.6}$$

Once labeled

$$\eta\,[\text{Pa/ppm}] = 0.089\,\frac{\text{m}}{\text{s}^2}\cdot m_{air}\left[\frac{\text{kg}}{\text{m}^2}\right] \tag{4.7}$$

relation (4.6) will take the form

$$p^{K}_{\text{CO}_2}\,[\text{Pa}] = \eta\,[\text{Pa/ppm}]\cdot c^{At}_{\text{CO}_2}\,[\text{ppm}] \tag{4.8}$$

or

$$c^{At}_{\text{CO}_2}\,[\text{ppm}] = \frac{1}{\eta\,[\text{Pa}/\text{ppm}]}\cdot p^{K}_{\text{CO}_2}\,[\text{Pa}]. \tag{4.9}$$

For the data in Table 1, after taking into account formulas (4.1) and (4.7), for individual layers and for a temperature in the cuvette T_K = 298 K (25°C), η takes the values given in Table 4.2.

Table 4.2. Values of parameter η for individual layers

Layer no.	m_{air} $\left[\frac{\text{kg}}{\text{m}^2}\right]$	η [Pa/ppm]
1	2151	191.4
2	1692	150.6
3	1284	114.3
4	1030	91.7
5	815	72.5
6	642	57.1
7	489	43.5

We can assume that in the considered layers of the troposphere we are dealing with pressure broadening, for which the width of the absorption line $\Delta\nu$ is proportional to the pressure p and inversely proportional to the root of the temperature T [28], that is, $\Delta\nu = C\frac{p}{\sqrt{T}}$ (C – constant). The same line width for a gas in a layer with temperature T_L and pressure p_L and a gas in a cuvette with temperature T_K and pressure p_K will be obtained when:

$$\Delta\nu = C\frac{p_K}{\sqrt{T_K}} = C\frac{p_L}{\sqrt{T_L}}.$$

Hence, in order for there to be the same line width in the cuvette and in the corresponding layer, the total pressure in the cuvette with temperature T_K should be:

$$p_K = p_L \cdot \sqrt{\frac{T_K}{T_L}}. \tag{4.10}$$

Thus, in the end, for a temperature in the cuvette of 298 K (25°C), the corresponding parameters in the subsequent layers and corresponding in the cuvette will take on the values shown in Table 4.3.

Table 4.3. Parameters of the gas mixture in the layers and in the cuvette

Layer no.	Height [km]	Average layer pressure p_L [Pa]	η [Pa/ppm]	Average temperature in the layer T_L [K]	$\sqrt{\frac{T_K}{T_L}}$	Corresponding cuvette pressure p_K [Pa]
1	0.5÷2.5	84950	191.4	278.5	1.034	87838
2	2.5÷4.5	66100	150.6	265.5	1.059	70000
3	4.5÷6.5	51500	114.3	252.5	1.086	55929
4	6.5÷8.5	40150	91.7	239.5	1.115	44767
5	8.5÷10.5	31100	72.5	226.5	1.147	35672
6	10.5÷12.5	23950	57.1	213.5	1.181	28285
7	12.5÷14.5	18400	43.5	200.5	1.219	22430

4.2. Direct measurements of thermal radiation after passing through CO_2–air mixtures for conditions corresponding to each layer

Experimental tests were carried out on a laboratory bench, the diagram of which is shown in Fig. 4.1.

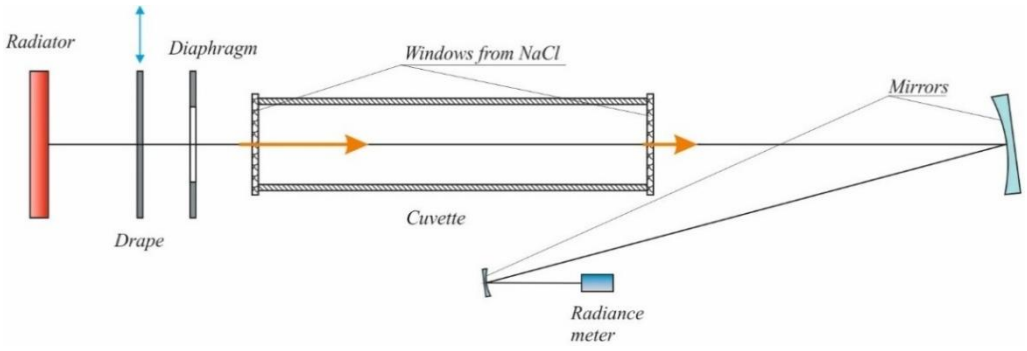

Fig. 4.1. Schematic of the experimental station

The stand consisted of a source of thermal radiation, which was a radiator in the form of a copper plate with corresponding holes in which electric heaters and a thermometer probe were placed. The radiating surface was covered with graphite. A view of the radiator is shown in Fig. 4.2.

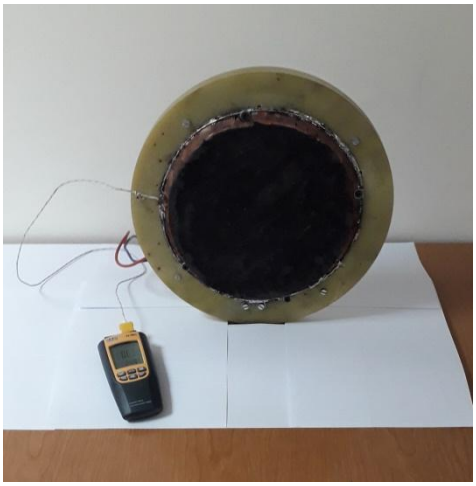

Fig. 4.2. View of the radiant heater with temperature gauge

Thermal radiation from this source was passed through a cuvette in the form of a thick-walled tube with an inner diameter of 140 mm and a length of 0.96 m enclosed by NaCl windows. A view of the cuvette is shown in Fig. 4.3.

Fig. 4.3. View of the cuvette

The cuvette, after pumping off, was first filled with carbon dioxide to a pressure at which its mass per unit area of the cuvette's cross-sectional area was equal to the mass of carbon dioxide per unit area in the corresponding layer. It was then "topped off" with air to the pressure corresponding to that layer according to Table 4.3. Small pressures of gas in the cuvette (less than 100 hPa) were measured with an oil manometer, while higher pressures were measured with a vacuometer. The relatively long plastic hoses used to supply carbon dioxide from the cylinder to the cuvette made it impossible to accurately fill the cuvette with this gas to a predetermined pressure, although once filled, its value was read relatively accurately (to the nearest 0.1 hPa).

The surface of the movable screen made of insulating material was covered with a layer of graphite, as was the surface of the heat sink. After the screen was removed, some of the thermal radiation passing through the 135-mm-diameter diaphragm opening passed through the cuvette and was focused onto the probe of the THORLABS PM200 radiation power meter by means of two mirrors. After inserting the screen, the meter was zeroed, and then the radiation power was measured after removing the screen. Measurements were taken alternately for a cuvette pumped out and filled with a mixture of air and carbon dioxide of the appropriate concentration. The temperature of the radiator plate was 63°C (336 K). The read radiation power incident on the power meter probe with the cuvette pumped off was – 285 μW (with the meter zeroed for the inserted aperture). The radiant power for each cuvette fill was measured five times, and then the two extreme values were discarded, and the arithmetic mean was calculated from the remaining three. The results of the quantities determined from the measurements are shown in Table 4.4, recording them in the following columns, respectively: c [ppm] – the concentration of CO_2 in the corresponding atmospheric layer determined from measurements of the partial pressure of CO_2 in the cuvette and Eq. (4.9), after entering the value of η from Table 4.3; I_{mj} – the radiation power value read on the meter for the conditions corresponding to the corresponding layer j.

Table 4.4. Stabelled relationships of measured radiant flux on CO_2 concentration in layers

c [ppm]	I_{m1} [μW]	c [ppm]	I_{m2} [μW]	c [ppm]	I_{m3} [μW]	c [ppm]	I_{m4} [μW]	c [ppm]	I_{m5} [μW]	c [ppm]	I_{m6} [μW]	c [ppm]	I_{m7} [μW]
0	285	0	285	0	285	0	285	0	285	0	285	0	285
8	278	10	274	24	273	29	276	28	278	24	279	32	278
15	270	22	270	45	268	66	270	60	271	39	274	54	277
25	265	37	268	124	258	111	261	154	265	83	271	104	272
41	262	56	264	222	255	221	255	377	255	134	267	181	267
46	262	107	259	355	252	331	253	489	254	213	264	233	265
147	252	242	252	488	248	488	253			319	259	361	262
306	247	512	247							497	257	512	262
449	242												

Given the fact that for the zero layer (up to 500 m), the temperature of the Earth's surface was assumed, according to the second law of thermodynamics, it was considered that the gases in the atmosphere up to this height, do not reduce the intensity of the thermal radiation of the Earth, so the consideration began with the 1st layer. Based on the results obtained, shown in Table 4.4, plots were made of the power of the measured thermal radiation as a function of CO_2 concentration for each layer, shown in Fig. 4.4.

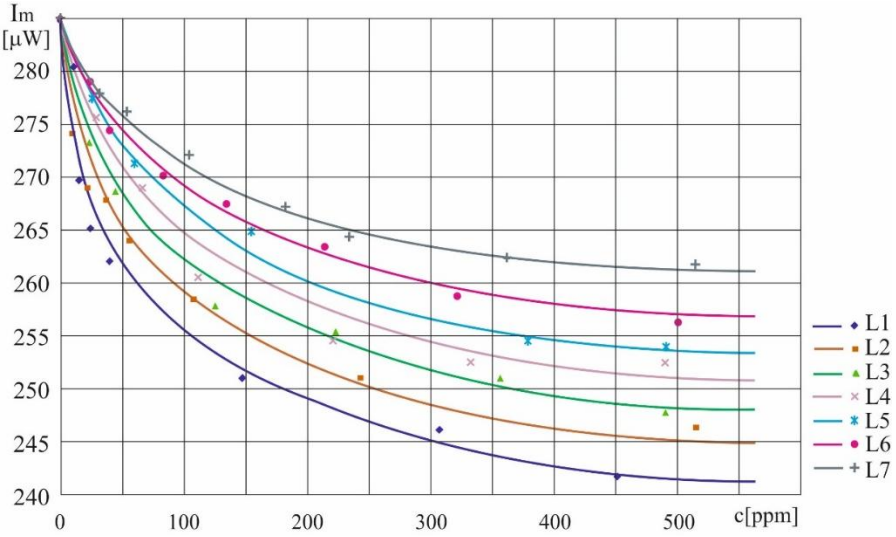

Fig. 4.4. Plots of the power of measured thermal radiation as a function of CO_2 concentration in the atmosphere for each layer

4.3. Development of measurement results

In order to further utilize the results of the measurements, the graphs in Fig. 4.4 were "crossed" with vertical lines to determine the values of radiant power for each layer at the same CO_2 concentrations, and dashed horizontal lines were drawn to read the minimum values of radiant power to which it asymptotically approaches with increasing concentration. This is shown in Fig. 4.5.

Based on the presented graphs, it can be concluded that in all layers for a sufficiently high concentration of CO_2, there is a clear saturation of the thermal radiation absorption process. The readings from the graphs taken are shown in Table 4.5.

When further utilizing the measurement results, it is necessary to interpret them correctly. First and foremost, the second law of thermodynamics must be taken into account

here. Let us recall that, in its simplest form, it means that a colder body cannot heat a warmer body or a body of the same temperature. This applies to all forms of energy transfer, including energy transfer through radiation. Let us consider a simple case shown in Fig. 4.6.

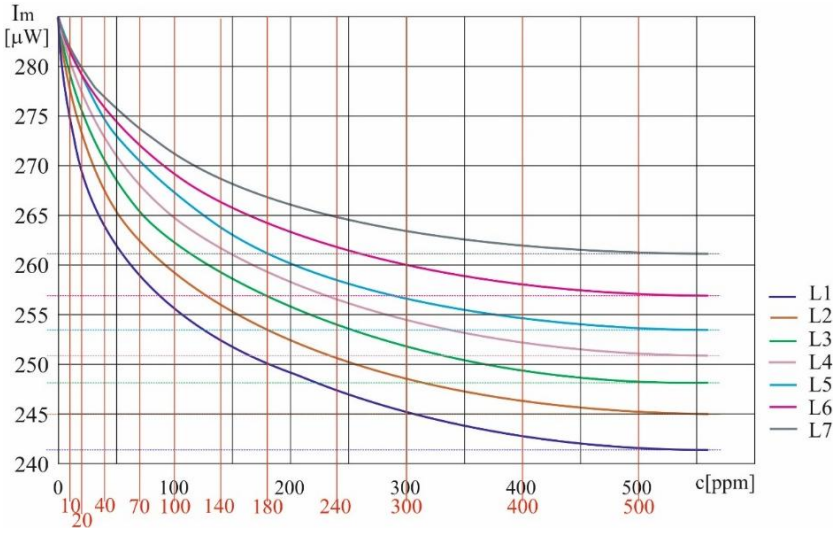

Fig. 4.5. Plots of thermal radiative power as a function of atmospheric CO_2 concentration, with vertical lines plotted for selected CO_2 concentrations and horizontal lines showing the lowest radiative power values in each layer

Table 4.5. Hypothetical thermal radiation power readings for a cuvette ith gas mixtures corresponding to conditions in each layer

c [ppm]	I_{m1} [μW]	I_{m2} [μW]	I_{m3} [μW]	I_{m4} [μW]	I_{m5} [μW]	I_{m6} [μW]	I_{m7} [μW]
0	285	285	285	285	285	285	285
10	275	278	279	281	282	282	282
20	270	273	276	278	279	279	280
40	264	268	270	273	275	276	277
70	259	262	266	268	270	272	274
100	256	259	262	265	267	269	271
140	253	256	259	262	264	266	269
180	250	254	257	259	261	264	267
240	248	251	254	257	258	262	265
300	245	249	252	255	257	260	264
400	243	247	250	253	255	258	262
500	242	245	249	251	254	257	261
$I_{m\min}$	241	245	248	251	254	257	261

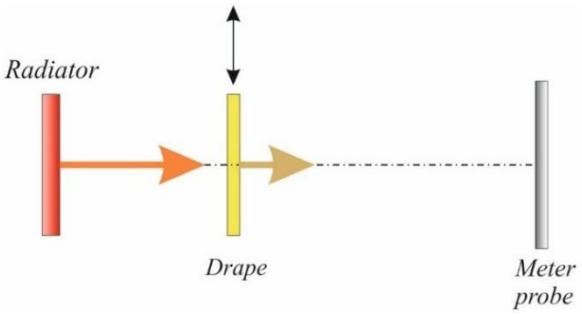

Fig. 4.6. Auxiliary figure for interpreting measurement results

A radiator with a temperature of T_{Rad} emits radiation that strikes a probe with a temperature of T_p. As a result, the probe is heated and changes its properties, allowing the radiation power to be determined on this basis. As a result, the probe is heated and changes its properties, allowing the radiation power to be determined on this basis. After inserting a drape with a T_{Dr} temperature equal to the probe temperature T_p, according to the second law of thermodynamics, the probe temperature cannot increase, even though, according to Boltzmann's law, the drape, like the radiator, also emits radiation that falls on the probe.

This is because the probe not only absorbs radiation but also emits it. This raises a fundamental question: if the meter was reset at an drape with a temperature of T_{Dr}, what does the reading on the meter mean when the drape is open? It seems obvious that this is the difference between the actual power of radiation emitted by the radiator and the power of radiation emitted by the drape.

Moving on to the experiment, note that for a laboratory temperature of 25°C (298 K) and a radiator temperature of 63°C (336 K) with an empty cuvette (no CO_2 in the layer) and the drape inserted, the meter was reset to zero. In fact, according to Boltzmann's law, the radiation emitted by the aperture of $I_{Dr} = \sigma \cdot (298\ \mathrm{K})^4$ had to fall on the meter probe. When the aperture was removed, radiation from the radiator $I_0^t = \sigma \cdot (336\ \mathrm{K})^4$ fell on the meter probe. Since the meter was zeroed with the aperture inserted, the measured radiation $I_{0m} = 285\ \mu\mathrm{W}$ was the difference of the actual radiation from the radiator and the drape.

$$I_{0m} = I_0^t - I_{Dr} = \sigma \cdot (336\ \mathrm{K})^4 - \sigma \cdot (298\ \mathrm{K})^4 = 285\ \mu\mathrm{W}. \tag{4.11}$$

(The σ-factor is assumed to be the same for the radiant and for the drape).

Based on (4.11)

$$\sigma = \frac{I_{0m}}{(336\ \mathrm{K})^4 - (298\ \mathrm{K})^4} = 5.86 \cdot 10^{-8}\ \mu\mathrm{W/K}^4.$$

Therefore, the radiation from the drape was:

$$I_{Dr} = \sigma \cdot (2998\,\mathrm{K})^4 = 462\,\mu\mathrm{W}.$$

The total actual radiation emitted by the heater was:

$$I_0^t = I_{0m} + I_{Dr} = \sigma \cdot 336\,\mathrm{K}^4 = 747\,\mu\mathrm{W}.$$

The saturation of the radiation absorption shown in the graphs (Figs. 4.4 and 4.5) allows us to divide the radiation used into I^A radiation with a spectrum that overlaps with the absorption (emission) spectrum of CO_2 and I^B radiation with a spectrum that does not (as was done in Chapter 3). Thus, after passing through the overexposed gas, the total radiation intensity will be:

$$I^t = I_0^B + I_0^A \cdot \tau(c) + I_{sp}^A(c), \tag{4.12}$$

τ(c) – radiation transmission I^A for a mixture of air and CO_2 with concentration c,
$I_{sp}^A(c)$ – intensity of spontaneous radiation emitted by CO_2 in the cuvette.

The proportion of I_0^A radiation to the total I_0^t radiation emitted by the radiator is

$$\Psi = \frac{I_0^A}{I_0^t} = \frac{I_0^A}{I_0^B + I_0^A}. \tag{4.13}$$

Hence

$$\left.\begin{aligned} I_0^A &= I_0^t \cdot \Psi \\ I_0^B &= I_0^t \cdot (1-\Psi) \end{aligned}\right\}. \tag{4.14}$$

Of course, what is measured is the total radiation reduced by the radiation at which the meter was zeroed, that is, the radiation for the inserted aperture. Therefore, its value is

$$I_m(c) = I_0^B + I_0^A \cdot \tau(c) + I_{sp}^A(c) - I_{Dr}. \tag{4.15}$$

It should be noted that the second law of thermodynamics also applies to the heating and cooling of gases. When the drape is inserted, there is equilibrium (the gas temperature is equal to the drape temperature), and the gas must emit the same amount of radiation that it absorbed. Spontaneous radiation "makes up for the shortfall" of radiation from the drape absorbed in CO_2. That is

$$I_{sp}^A(c) = I_{Dr}^A \cdot (1-\tau(c)). \tag{4.16}$$

Furthermore, as with the radiator, it is now necessary to divide the radiation into radiation absorbable by CO_2, I_{Dr}^A, and radiation not absorbable by this gas, I_{Dr}^B.

In addition, analogous to the radiator, was entered

$$I_{Dr}^{A} = I_{Dr} \cdot \Psi, \quad I_{Dr}^{B} = I_{Dr} \cdot (1-\Psi). \tag{4.17}$$

After substituting (4.17) into (4.16), the following is obtained

$$I_{sp}^{A}(c) = I_{Dr} \cdot \Psi \cdot (1-\tau(c)). \tag{4.18}$$

After substitution into (4.15)

$$I_{m}(c) = I_{0}^{t} \cdot (1-\Psi) + I_{Dr} \cdot \Psi - I_{Dr} + \tau(c) \cdot \Psi \cdot (I_{0}^{t} - I_{Dr}). \tag{4.19}$$

Hence

$$\tau(c) = \frac{I_{m}(c) - (I_{0}^{t} - I_{Dr})(1-\Psi)}{\Psi \cdot (I_{0}^{t} - I_{Dr})}. \tag{4.20}$$

After substituting the determined values: I_0^t = 747 μW, I_{Dr} = 462 μW, $I_0^t - I_{Dr}$ = 285 μW, the absorptive radiation transmission value I^A in the cuvette is

$$\tau(c) = \frac{I_{m}(c) - 285\,\mu\text{W}\,(1-\Psi)}{\Psi \cdot 285\,\mu\text{W}}. \tag{4.21}$$

Figures 4.2 and 4.3 show that for sufficiently large values of CO_2 concentration, the graphs turn into horizontal lines. It follows that the absorbable radiation has been completely absorbed that is, for sufficiently large values of the concentration of c, $\tau(c) = 0$ and Eq. (4.21) will take the form of equation

$$I_{m_{\min}}(c) = 285\,\mu\text{W}(1-\Psi) = 0.$$

Hence

$$\Psi = 1 - \frac{I_{m_{\min}}}{285\,\mu\text{W}}. \tag{4.22}$$

Based on the graphs in Fig. 4.5, the Ψ_L contribution of absorptive radiation I^A to the total radiation for each layer L was determined and is shown in Table 4.6.

Table 4.6. Share of absorbable radiation I^A in total radiation for each layer L

L	1	2	3	4	5	6	7
$I_{m_{\min}}$	241	245	248	251	254	257	261
Ψ_L	0.154	0.140	0.130	0.119	0.109	0.098	0.084

It should be noted that the values of Ψ_L are associated with the respective layers and do not depend on the concentration c. Therefore, by inserting them into Eq. (4.21) and using the data in Table 4.5, we can determine the transmission τ of absorptive radiation I^A in individual layers for specific concentrations c of CO_2. The results obtained in this way are shown in Table 4.7.

Table 4.7. Transmission $\tau(c)$ of absorptive radiation I^A in individual layers

c [ppm]	τ_1	τ_2	τ_3	τ_4	τ_5	τ_6	τ_7
0	1.000	1.000	1.000	1.000	1.000	1.000	1.000
10	0.772	0.825	0.838	0.882	0.903	0.893	0.875
20	0.658	0.699	0.757	0.794	0.807	0.785	0.791
40	0.522	0.574	0.595	0.646	0.678	0.678	0.666
70	0.408	0.424	0.487	0.499	0.517	0.535	0.541
100	0.339	0.348	0.379	0.410	0.421	0.427	0.415
140	0.271	0.273	0.298	0.322	0.324	0.320	0.332
180	0.203	0.223	0.244	0.233	0.227	0.248	0.248
240	0.157	0.148	0.163	0.174	0.131	0.177	0.165
300	0.089	0.098	0.109	0.115	0.099	0.105	0.123
400	0.043	0.048	0.055	0.056	0.034	0.033	0.039
500	0.020	0.001	0.028	0.001	0.002	0.001	0.001

These results have been plotted on a graph (Fig. 4.7).

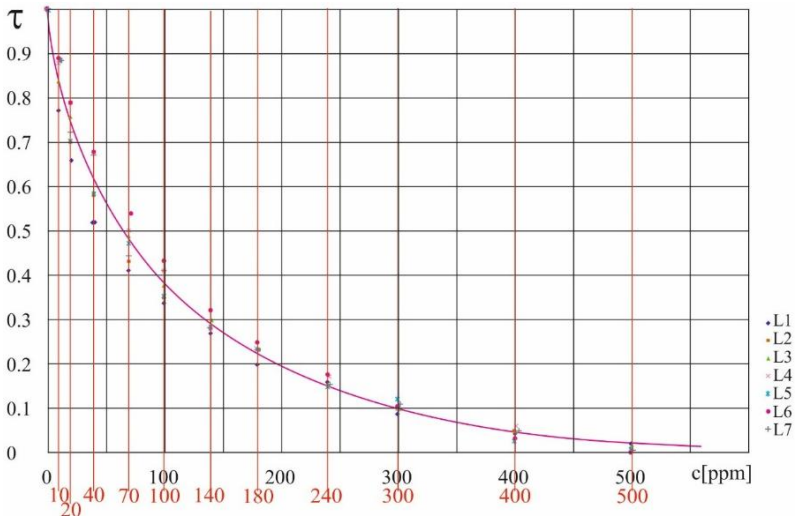

Fig. 4.7. Averaged transmission plot of absorptive radiation I^A in all layers

From the plotted points on the graph, it can be seen that the transmittance of absorbable radiation in the different layers for the same CO_2 concentrations is similar. This is most likely due to the fact that the active cross-section for absorption is inversely proportional to pressure, and therefore, at the same concentration, despite the decrease in absorbing mass in higher layers, the absorption coefficient for absorbable radiation does not change. Therefore, a graph was made for the averaged values of τ transmission and the values of this parameter were read from it for the corresponding values of CO_2 concentration. The results are shown in Table 4.8.

Table 4.8. Averaged transmission $\tau(c)$ of absorptive radiation for all layers

c [ppm]	0	10	20	40	70	100	140	180	240	300	400	500
$\tau(c)$	1.00	0.84	0.75	0.62	0.48	0.38	0.29	0.22	0.15	0.10	0.05	0.02

Inserting the data from Tables 4.6 and 4.8 into Eq. (4.18), the values of spontaneous radiation intensity for all layers at 25°C were obtained for selected values of CO_2 concentrations. The results are shown in Table 4.9.

Table 4.9. Spontaneous radiation intensity values for all layers at 25°C for selected CO_2 concentration values

c [ppm]	τ	$I^A_{sp_1}$ [μW]	$I^A_{sp_2}$ [μW]	$I^A_{sp_3}$ [μW]	$I^A_{sp_4}$ [μW]	$I^A_{sp_5}$ [μW]	$I^A_{sp_6}$ [μW]	$I^A_{sp_7}$ [μW]
0	1.00	0.0	0.0	0.0	0.0	0.0	0.0	0.0
10	0.84	11.4	10.4	9.6	8.8	8.1	7.3	6.2
20	0.75	17.8	16.2	15.0	13.8	12.6	11.3	9.7
40	0.62	27.0	24.5	22.8	20.9	19.1	17.2	14.7
70	0.48	37.0	33.6	31.2	28.6	26.2	23.5	20.2
100	0.38	44.1	40.1	37.2	34.1	31.2	28.0	24.0
140	0.29	50.5	45.9	42.6	39.0	35.8	32.1	27.5
180	0.22	55.5	50.4	46.8	42.9	39.3	35.3	30.2
240	0.15	60.5	55.0	51.1	46.8	42.8	38.5	33.0
300	0.10	64.0	58.2	54.0	49.5	45.3	40.7	34.9
400	0.05	67.6	61.4	57.1	52.3	47.9	43.0	36.8
500	0.02	69.7	63.4	58.8	53.9	49.3	44.3	38.0

In real conditions, the radiator is the surface of the Earth, for which an average temperature of 15°C (288 K) is assumed. If a radiator of this temperature were used under the conditions of the experiment conducted, the flux of radiation used would have a value of

$$I_E = \sigma \cdot (288\,\mathrm{K})^4 = 5.86 \cdot 10^{-8}\,\frac{\mu\mathrm{W}}{\mathrm{K}^4} \cdot (288\,K)^4 = 403\,\mu\mathrm{W}.$$

Therefore, this value was defined as 100 relative units (r.u.) and was used later in the paper by replacing the

$$I\,[\mu\mathrm{W}] = \frac{100}{403} \cdot I\,[\mathrm{r.u.}] = 0.248 \cdot I\,[\mathrm{r.u.}]. \tag{4.23}$$

The values of spontaneous radiation for individual layers at 25°C (Table 4.9) in assumed relative units are shown in Table 4.10.

Table 4.10. Values of spontaneous radiation intensity in all layers for selected values of CO_2 concentrations at 25°C in relative units

c [ppm]	τ	$I^A_{sp_1}$ [r.u.]	$I^A_{sp_2}$ [r.u.]	$I^A_{sp_3}$ [r.u.]	$I^A_{sp_4}$ [r.u.]	$I^A_{sp_5}$ [r.u.]	$I^A_{sp_6}$ [r.u.]	$I^A_{sp_7}$ [r.u.]
0	1.00	0.00	0.00	0.00	0.00	0.00	0.00	0.00
10	0.84	2.83	2.58	2.38	2.18	2.01	1.81	1.54
20	0.75	4.41	4.02	3.72	3.42	3.12	2.80	2.41
40	0.62	6.70	6.08	5.65	5.18	4.74	4.27	3.65
70	0.48	9.18	8.33	7.74	7.09	6.50	5.83	5.01
100	0.38	10.94	9.94	9.23	8.46	7.74	6.94	5.95
140	0.29	12.52	11.38	10.56	9.67	8.88	7.96	6.82
180	0.22	13.76	12.50	11.61	10.64	9.75	8.75	7.49
240	0.15	15.00	13.64	12.67	11.61	10.61	9.55	8.18
300	0.10	15.87	14.43	13.39	12.28	11.23	10.09	8.66
400	0.05	16.76	15.23	14.16	12.97	11.88	10.66	9.13
500	0.02	17.29	15.72	14.58	13.37	12.23	10.99	9.42

In order for the model to be adequate to reality, temperature differences between laboratory and actual conditions in each layer still need to be taken into account. Therefore, for the temperatures of interest, the concentration of excited CO_2 molecules has been taken into account because both in the emission and absorption of thermal radiation, there are oscillation-rotation transitions in these molecules. Taking into account the absorption spectrum of CO_2 adopted from the HITRAN database, the concentration of molecules excited to the lowest oscillatory levels was considered. Based on [29], the energy of these levels is respectively:

01^10 – 667.3 cm^{-1} = $1.328 \cdot 10^{-20}$ J,
02^00 – 1285.8 cm^{-1} = $2.559 \cdot 10^{-20}$ J,
10^00 – 1388.1 cm^{-1} = $2.762 \cdot 10^{-20}$ J,
03^10 – 1931.9 cm^{-1} = $3.844 \cdot 10^{-20}$ J.

To this energy must be added the rotational energy of the molecules, which is expressed by the formula

$$E_r = Bhcj(j+1), \tag{4.24}$$

where:

$h = 6.63 \cdot 10^{-34}$ Js – Planck's constant,

$c = 3 \cdot 10^{10}$ cms^{-1} – speed of light in vacuum,

j – rotational number of a molecule.

The rotational constant B is similar for all the lowest oscillatory levels and according to [25] is $B = 0.39$ cm^{-1}.

The distribution of concentration of molecules with respect to rotational levels for the oscillatory level v is expressed by the formula:

$$nvj \cong N_v \left(\frac{2hcB}{kT} \right) (2j+1) \exp\left[-F(j) \frac{hc}{kT} \right], \tag{4.25}$$

where

$$F(j) \approx B_v j(j+1). \tag{4.26}$$

The maximum concentration of excited molecules is temperature dependent and occurs for rotational quantum number

$$j_{\max} = \sqrt{\frac{k \cdot T}{2Bhc}} - \frac{1}{2}. \tag{4.27}$$

After substituting the assumed numerical values into Eq. (4.27)

$$j_{\max} = 0.943\,\mathrm{K}^{-1/2} \cdot \sqrt{T} - \frac{1}{2}. \tag{4.28}$$

According to Eq. (4.24), the rotational energy of the molecules for each quantum number j varies, but in the model presented here, a simplification was adopted by taking the rotational energy of all molecules from the oscillatory level v, equal to the rotational energy for the number $j_{\max}$, which was considered to be close to the average rotational energy at this oscillatory level.

Due to the fact that the temperatures in each layer and in the laboratory are different, $j_{\max}$ was determined for the considered conditions based on Eq. (4.28), and from Eq. (4.24), the rotational energy adopted for them was calculated. The results are shown in Table 4.11.

Table 4.11. The rotational quantum number j_{max}, the corresponding rotational energy E_r and the total energy of the lowest oscillatory levels E_{vr} of the CO_2 molecule

Layer no.	Average temperature in the layer T_L [K]	j_{max}	E_r [cm^{-1}]	E_v [cm^{-1}]			E_{vr} [cm^{-1}]		
				01^10	02^00	10^00	01^10	02^00	10^00
Lab	298	16	106	667	1286	1388	773	1392	1494
0	287	15	94				761	1380	1482
1	278.5	15	94				761	1380	1482
2	265.5	15	94				761	1380	1482
3	252.5	14	82				749	1368	1470
4	239.5	14	82				749	1368	1470
5	226.5	14	82				749	1368	1470
6	213.5	13	71				738	1357	1459
7	200.5	13	71				738	1357	1459

According to Boltzmann's law, the concentration of molecules excited to a level with energy E_j is

$$n_j = n \cdot \frac{e^{-\frac{E_j}{kT}}}{q(T)}, \tag{4.29}$$

where

k – Planck's constant,
T – temperature,
n – concentration of all CO_2 molecules

$$q(T) = \sum_j e^{-\frac{E_j}{kT}}. \tag{4.30}$$

For a temperature of 25°C (298 K)

$$q(T) = \sum_j e^{-\frac{E_j}{kT}} = 1 + 0.0238 + 0.0012 + 0.0007 = 1.026.$$

The concentration of non-excited molecules is then

$$n_0 = n \cdot \frac{1}{1.026} = 0.975 \cdot n.$$

Obviously, at the lower temperatures found in the atmosphere, n_0 is even closer to n, and thus lowering the temperature in the higher layers of the atmosphere has virtually no effect on the increase in the concentration of absorbing (non-excited) molecules, and thus cannot noticeably affect the increase in radiation absorption.

Spontaneous radiation, on the other hand, is associated with excited molecules and can be assumed to be proportional to the concentration of these molecules.

Analogously as for the zero level, taking from Table 4.11 the oscillation-rotation energy of CO_2 molecules at the lowest levels and using formula (4. 29), the ratio of the concentration of excited molecules at oscillation levels 01^10, 02^00, 10^00 denoted by n_1, n_2, n_3, respectively, and the concentration of excited molecules at all levels denoted by n^*, to the concentration of all molecules n was determined for the temperature in the laboratory (298 K) and the temperatures in the different layers of the atmosphere (n^*/n). In addition, it was determined how many times the concentration of excited molecules in each layer decreased as a result of the lower temperature compared to the temperature in the laboratory $\left(\frac{n^*}{n^*_{Lab}}\right)$. The results are shown in Table 4.12.

Table 4.12. The ratio of the concentration of excited molecules at individual levels n_j to all molecules n, excited molecules n^* to all molecules n, and the ratio of the concentration of excited molecules in individual layers to the concentration of excited molecules in the laboratory $\left(\frac{n^*}{n^*_{Lab}}\right)$

Layer no.	n_1/n	n_2/n	n_3/n	n^*/n	$\left(\frac{n^*}{n^*_{Lab}}\right)$
Lab	0.0234	0.0010	0.0010	0.0254	1.000
0	0.0215	0.0010	0.0010	0.0235	0.925
1	0.0186	0.0010	0.0000	0.0196	0.772
2	0.0157	0.0010	0.0000	0.0167	0.657
3	0.0138	0.0000	0.0000	0.0138	0.543
4	0.0109	0.0000	0.0000	0.0109	0.429
5	0.0079	0.0000	0.0000	0.0079	0.311
6	0.0070	0.0000	0.0000	0.0070	0.276
7	0.0050	0.0000	0.0000	0.0050	0.197

It was assumed that the intensity of spontaneous radiation is proportional to the concentration of excited molecules. Therefore, based on the data in Tables 4.10 and 4.12, the intensity of spontaneous radiation in individual layers at real temperatures was determined for selected CO_2 concentrations. The results are shown in Table 4.13.

Table 4.13. Spontaneous radiation intensity values in all layers for selected values of CO_2 concentrations at actual temperatures

c [ppm]	$I^A_{sp_1}$ [r.u.]	$I^A_{sp_2}$ [r.u.]	$I^A_{sp_3}$ [r.u.]	$I^A_{sp_4}$ [r.u.]	$I^A_{sp_5}$ [r.u.]	$I^A_{sp_6}$ [r.u.]	$I^A_{sp_7}$ [r.u.]
0	0.00	0.00	0.00	0.00	0.00	0.00	0.00
10	2.18	1.70	1.29	0.94	0.63	0.50	0.30
20	3.40	2.64	2.02	1.47	0.97	0.77	0.47
40	5.17	4.00	3.07	2.22	1.47	1.18	0.72
70	7.08	5.48	4.21	3.04	2.02	1.61	0.99
100	8.44	6.54	5.01	3.63	2.41	1.91	1.17
140	9.66	7.48	5.74	4.15	2.76	2.19	1.34
180	10.62	8.22	6.31	4.57	3.03	2.41	1.47
240	11.58	8.97	6.88	4.98	3.30	2.63	1.61
300	12.25	9.49	7.27	5.27	3.49	2.78	1.71
400	12.93	10.01	7.69	5.57	3.69	2.94	1.80
500	13.34	10.34	7.92	5.74	3.80	3.03	1.85

4.4. Effect of successive atmospheric layers on the intensity of Earth's cooling radiation

The described experimental studies and the analysis carried out make it possible to quantify the percentage dependence of the Earth's space-emitted cooling thermal radiation on the concentration of CO_2 in the atmosphere. The idea of this method is explained on the example of the three-layer model shown in Fig. 4.8 using the assumptions made in Chapter 3.

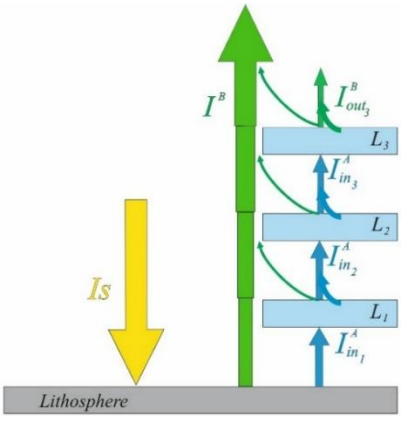

Fig. 4.8. Schematic demonstration of radiation transfer through successive layers of the atmosphere in the three-layer model

In this model, solar radiation I_S heats the surface of the lithosphere, and this, having a certain temperature, emits thermal radiation I_{in}. This radiation can be divided into radiation absorbed by CO_2, I^A, and radiation not absorbed by CO_2, I^B. The share of I^A radiation in the total radiation emitted by the Earth's surface depends, among other things, on the width of the absorption lines of the absorbing gas, and thus on its pressure and temperature. It is larger in the lower layers of the atmosphere, where the lines are wider, and smaller in the higher layers. In the first layer, I^A radiation decreases due to absorption by CO_2 and increases due to spontaneous emission from this gas, while I^B radiation remains unchanged. After passing through the first layer, the value of absorbable radiance changes $(I^A_{out_1} \neq I^A_{in_1})$ while the value of non-absorbable radiance remains the same $(I^B_{out_1} \neq I^B_{in_1})$. Then, in the second layer, due to the narrowness of the line, the proportion of I^A radiation is smaller, and therefore some of this radiation, after leaving the first layer, will become I^B radiation for the second layer. Thus, we have $(I^A_{in_2} < I^A_{out_1})$ end $(I^B_{in_2} \neq I^B_{out_1})$. In this layer, as in the first layer, the radiation $I^A_{in_2}$ decreases due to absorption by CO_2 and increases due to spontaneous emission, while the radiation $(I^B_{in_2} = I^B_{out_2})$. Similarly, in the case of the third layer, the fraction of I^A radiation in the total radiation is smaller than in the case of the second layer, so again some of this radiation will become I^B radiation for the third layer. Eventually, all the $I^A_{out_3}$ radiation from the last layer, along with the $I^B_{out_3}$ radiation as the total I_{out} radiation, will leave the atmosphere and be the radiation that cools our planet.

The idea presented with this three-layer model was used to quantitatively describe the phenomena of interest in an eight-layer model. The assumption mentioned in Subsection 4.1 was made that up to an altitude of 500 m, the atmosphere has an Earth surface temperature of 15°C (288 K). With this assumption, according to the second law of thermodynamics, gases that absorb the Earth's thermal radiation must emit the same radiative power and thus become neutral gases. Therefore, the consideration began with layer one with a temperature lower than that of the Earth's surface.

As assumed in Subsection 4.3, the total thermal radiation from the Earth entering this layer is I^t_0 = 100 r.u. The proportion of absorptive radiation in this layer, according to Table 4.4, is Ψ_1 = 0.154. Therefore, absorptive radiation enters the layer with a value of

$$I^A_{in_1} = \Psi_1 \cdot I^t_0 = 0.154 \cdot I^t_0 \tag{4.31}$$

and non-absorbing radiation of

$$I^B_{in_1} = (1 - \Psi_1) \cdot I^t_0 = 0.846 \cdot I^t_0. \tag{4.32}$$

As described in the three-layer model, absorbable radiation decreases in value due to absorption and increases due to spontaneous emission. Consequently, its value at the output of the first layer should be

$$I^A_{out_1}(c) = \Psi_1 \cdot I^t_0 \cdot \tau(c) + I^A_{sp_1}(c) = 15.4 \text{ r.u.} \cdot \tau(c) + I^A_{sp_1}(c). \tag{4.33}$$

On the other hand, the value of the intensity of non-absorbable radiation does not change and, after passing through the first layer, continues to be

$$I^B_{out_1} = I^B_{in_1} = 84.6 \text{ r.u.} \tag{4.34}$$

The total radiation after passing through the first layer will have a value of

$$I_{out_1}(c) = I^A_{out_1}(c) + I^B_{out_1}. \tag{4.35}$$

Based on the formulas presented, using Table 4.12, the radiant intensity values after the first layer, shown in Table 4.14, were determined.

Table 4.14 Radiant intensity values behind the first layer for specific CO_2 concentrations in the atmosphere

c [ppm]	τ	$I^A_{sp_1}$ [r.u.]	$I^A_{out_1}(c)$ [r.u.]	$I_{out_1}(c)$ [r.u.]
0	1.00	0.00	15.40	100.00
10	0.84	2.18	15.12	99.72
20	0.75	3.40	14.95	99.55
40	0.62	5.17	14.72	99.32
70	0.48	7.08	14.47	99.07
100	0.38	8.44	14.29	98.89
140	0.29	9.66	14.13	98.73
180	0.22	10.62	14.01	98.61
240	0.15	11.58	13.89	98.49
300	0.10	12.25	13.79	98.39
400	0.05	12.93	13.70	98.30
500	0.02	13.34	13.65	98.25

It should be noted that Table 4.6, determining the proportion of absorptive radiation in each layer, referred to thermal radiation with a spectrum not distorted by the selectively absorbing gases through which the radiation passes. Therefore, before moving to the second layer, it is necessary to determine the value of the intensity of the hypothetical radiation behind the first layer containing the actual value of the absorbable radiation and the undistorted spectrum. The intensity value of this radiation is

$$I_1^{tf}(c) = \frac{I_{out_1}^A(c)}{\Psi_1}. \tag{4.36}$$

Thus, the absorptive radiation entering the second layer is

$$I_{in_2}^A(c) = \Psi_2 \cdot I_1^{tf}(c) = 0.140 \cdot I_1^{tf}(c). \tag{4.37}$$

Analogous to the first layer, the absorptive radiation coming out of the second layer can be determined by the formula

$$I_{out_2}^A(c) = I_{in_2}^A(c) \cdot \tau(c) + I_{sp_2}^A(c). \tag{4.38}$$

In contrast, the non-absorbable radiation in the second layer, due to the decrease in the proportion of absorbable radiation, will increase to a value of

$$I_{out_2}^B = I_{out_1}^B + (\Psi_1 - \Psi_2) \cdot I_1^{tf}(c). \tag{4.39}$$

The total radiation after exiting the second layer, analogous to that after exiting the first layer, can be written with the formula

$$I_{out_2}(c) = I_{out_2}^A(c) + I_{out_2}^B(c). \tag{4.40}$$

The final irradiance values, relating to the second layer, are recorded in Table 4.15.

Table 4.15. Radiant intensity values for the second layer

c [ppm]	$\tau(c)$	$I_1^{tf}(c)$ [r.u.]	$I_{sp_2}^A(c)$ [r.u.]	$I_{out_2}^A(c)$ [r.u.]	$I_{out_2}^B(c)$ [r.u.]	$I_{out_2}(c)$ [r.u.]
0	1.00	100.00	0.00	14.00	86.00	100.00
10	0.84	98.18	1.70	13.25	85.97	99.22
20	0.75	97.08	2.64	12.83	85.96	98.79
40	0.62	95.58	4.00	12.30	85.94	98.24
70	0.48	93.96	5.48	11.79	85.92	97.71
100	0.38	92.79	6.54	11.48	85.90	97.38
140	0.29	91.75	7.48	11.21	85.88	97.09
180	0.22	90.97	8.22	11.02	85.87	96.89
240	0.15	90.19	8.97	10.86	85.86	96.72
300	0.10	89.55	9.49	10.74	85.85	96.59
400	0.05	88.96	10.01	10.63	85.85	96.48
500	0.02	88.64	10.34	10.59	85.84	96.43

In general, the value of the intensity of the hypothetical radiation coming out of layer $j-1$ is

$$I_{j-1}^{tf}(c) = \frac{I_{out_{j-1}}^{A}(c)}{\Psi_{j-1}}. \tag{4.41}$$

Absorbable radiation entering layer j

$$I_{in_j}^{A}(c) = \Psi_j \cdot I_{j-1}^{tf}(c). \tag{4.42}$$

Absorbable radiation coming out of layer j

$$I_{out_j}^{A}(c) = I_{in_j}^{A}(c) \cdot \tau(c) + I_{sp_j}^{A}(c). \tag{4.43}$$

Non-absorbent radiation in layer j

$$I_{out_j}^{B} = I_{out_{j-1}}^{B} + (\Psi_{j-1} - \Psi_j) \cdot I_{j-1}^{tf}(c). \tag{4.44}$$

The formulas presented here made it possible to determine the value of total radiations behind successive layers for specific CO_2 concentrations in the atmosphere for the eight-layer model. They are presented in Table 4.16.

Table 4.16. Values of total radiations behind successive layers for specific CO_2 concentrations in the atmosphere

c[ppm]	$I_{out1}(c)$ $[r.u.]$	$I_{out2}(c)$ $[r.u.]$	$I_{out3}(c)$ $[r.u.]$	$I_{out4}(c)$ $[r.u.]$	$I_{out5}(c)$ $[r.u.]$	$I_{out6}(c)$ $[r.u.]$	$I_{out7}(c)$ $[r.u.]$
0	100.00	100.00	100.00	100.00	100.00	100.00	100.00
10	99.72	99.22	98.54	97.77	96.95	96.27	95.65
20	99.55	98.79	97.83	96.80	95.72	94.88	94.15
40	99.32	98.24	96.97	95.66	94.35	93.48	92.73
70	99.07	97.71	96.22	94.76	93.36	92.54	91.81
100	98.89	97.38	95.78	94.27	92.83	92.08	91.37
140	98.73	97.09	95.44	93.90	92.44	91.77	91.07
180	98.61	96.89	95.22	93.67	92.21	91.60	90.89
240	98.49	96.72	95.03	93.48	92.01	91.48	90.77
300	98.39	96.59	94.89	93.35	91.87	91.38	90.67
400	98.30	96.48	94.79	93.24	91.76	91.32	90.58
500	98.25	96.43	94.72	93.18	91.70	91.28	90.52

Since, in the relative units adopted, the Earth's surface emits radiation with an intensity of 100 units, the radiation intensity values given in Table 4.16 specify the percentage of radiation leaving successive layers in the radiation emitted by the Earth's surface.

Therefore, in the rest of the paper, relative units are replaced by percentages in the graphs. Figure 4.9, based on Table 4.16, shows the aforementioned dependence of the percentage of radiation leaving successive layers in the radiation emitted by the Earth's surface on the concentration of CO_2 in the atmosphere.

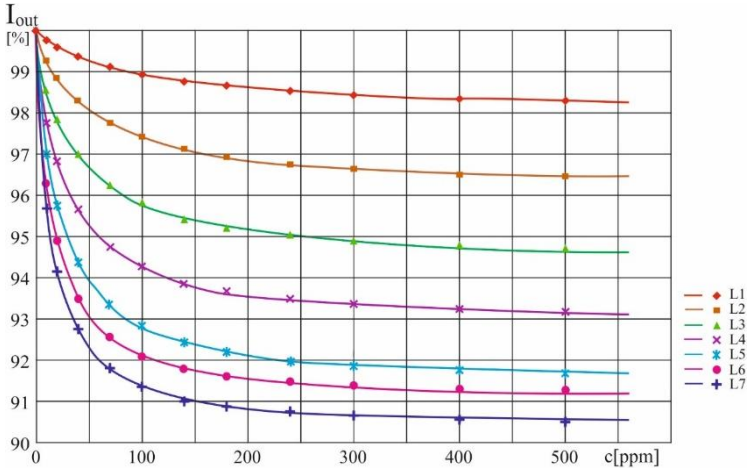

Fig. 4.9. Dependence of the percentage of radiation leaving successive layers in the radiation emitted by the Earth's surface on the concentration of CO_2 in the atmosphere

Ultimately, however, what is of interest is how the entire atmosphere reduces the Earth's thermal radiation emissions. This is determined by the percentage of radiation leaving the last, seventh layer (Fig. 4.10).

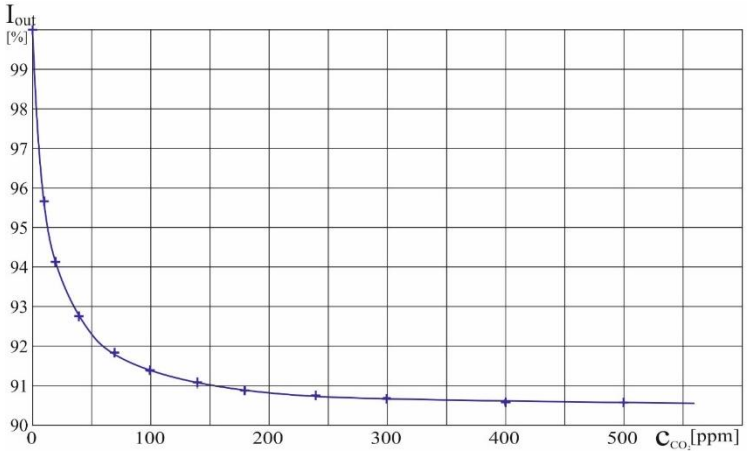

Fig. 4.10. Dependence of the percentage of radiation emitted to space in the radiation emitted by the Earth's surface on the concentration of CO_2 in the atmosphere

It is also possible to determine the percentage decrease in the Earth's thermal radiation emission to space, defined as $\Delta I_{out}(c) = 100\% - I_{out}(c)$ and shown in Table 4.17.

Table 4.17. Percentage decrease in Earth's thermal radiation to space by CO_2 in the atmosphere

c [ppm]	0	10	20	40	70	100	140	180	240		300	400	500
$I_{out}(c)$ [%]	100	95.65	94.15	92.73	91.81	91.37	91.07	90.89	90.77		90.67	90.58	90.52
$\Delta I_{out}(c)$ [%]	0	4.35	5.85	7.27	8.19	8.63	8.93	9.11	9.23		9.33	9.42	9.48

These results are shown in the graph (Fig. 4.11).

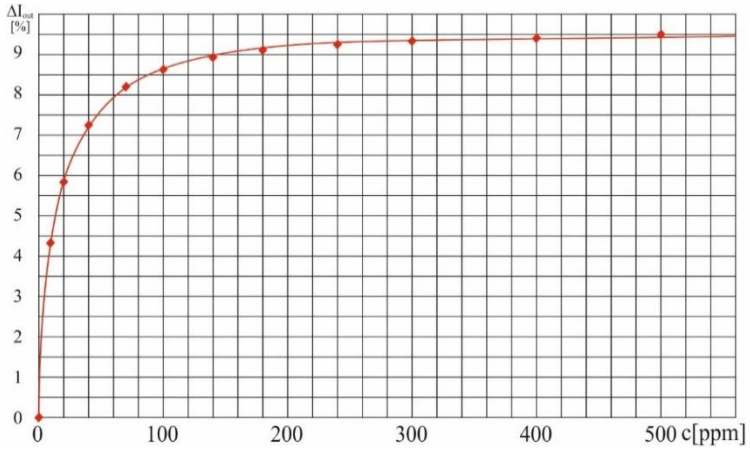

Fig. 4.11. Percentage of decrease in Earth's thermal radiation from CO_2 across the atmosphere

4.5. Conclusions of the eight-layer model

The final graph shown in Fig. 4.10 shows that carbon dioxide in the atmosphere, even at very high concentrations, can only reduce the emission of cooling thermal radiation to space by less than 10%. The graph also shows that already at CO_2 concentrations below 150 ppm, we have virtually saturated the decrease in the emission of this radiation, and thus further increases in this concentration have virtually no significant effect on the described decrease.

The presented model of the atmosphere takes into account the influence of pressure and temperature on the width of absorption lines. The second law of thermodynamics is taken into account in radiative energy transfer processes. Using spontaneous radiation, radiation re-emission processes were taken into account.

When measuring the intensity of radiation passing through actual gases in a cuvette at an absorbance comparable to that in the atmosphere, it was impossible to ignore the broadening of the absorption lines resulting from the peak saturating faster than the wings. Therefore, the model presented should correspond to actual conditions. As already noted in Subsection 2.6, including water vapor and other gases with absorption spectra partially overlapping with that of CO_2 in the model would result in faster saturation of radiation absorption. This means that, in reality, even at lower concentrations of this gas than those shown in the study, an increase in CO_2 concentration has no effect on the increase in atmospheric temperature.

Based on the considerations in Chapter 3, the model omits back radiation. It was decided that this radiation is not a direct cooling factor for our planet and that its contribution to the vertical temperature distribution in the atmosphere, which may affect radiation emissions into space, is very small compared to the influence of vertical air movements or phase changes of water in the atmosphere.

Ultimately, therefore, analysis using reliable experimental results proves that the slight effect of increased CO_2 concentrations in the atmosphere on changes in Earth's temperature would be significant if its value were less than 100 ppm, which is many times less than the current concentration.

5. Summary and final conclusions

The material presented here, based directly or indirectly on the results of experiments and on the conclusions of these experiments and on the laws of physics, shows unequivocally that the mass of carbon dioxide in the Earth's atmosphere is far greater than the so-called saturation mass, above which the further introduction of this gas into the atmosphere cannot affect any warming of the atmosphere. In Chapter 3, based on experimental facts, it was shown that the share of CO_2-absorbable radiation in the entire Earth's thermal radiation is small. It is clear from the principle of conservation of energy that once a sufficiently large mass of CO_2 is introduced into the atmosphere, that is, once a certain concentration of CO_2 is exceeded, the Earth's thermal radiation will no longer be absorbed due to the practically complete absence of its absorbable component. Chapter 4 considers the eight-layer model, taking into account data obtained directly from the experiment. This took into account the spontaneous radiation emitted by carbon dioxide in the atmosphere, as well as the effect of reduced temperature in the higher layers on the decrease in thermal radiation emission to space. The results completely confirm the conclusions of Chapter 3, that with the current concentration of CO_2 in the atmosphere, we have full saturation of the absorption of the Earth's thermal radiation by this gas, and thus an additional increase in its concentration in the atmosphere cannot cause an increase in temperature. Thus, an important factual question arises. **Where is the error in the commonly accepted reasoning from which it follows that an additional increase in the concentration of CO_2 in the atmosphere must lead to a significant increase in the temperature of our planet?**

In the vast majority of articles in climatology, authors, starting with Svante Arrhenius [2], take for granted the effect of CO_2 on the increase in atmospheric temperature. There are a number of works mentioned in Chapter 2, in which the authors, using computer circulation models and adopting data from the HITRAN database, from measurement points and from satellite images, try to prove the assumed thesis about the effect of CO_2 concentration on atmospheric temperature. The conclusions of Ångström's work are rejected, and the assumption is mostly implicitly made that, at sufficiently high concentrations, all of the thermal radiation emitted by the Earth can be absorbed by carbon dioxide. Such an approach was made, among others, by the well-known Japanese physicist, climatologist and meteorologist from Princeton University Syukuro Manabe, who

in his work [22], using a simple model of the general circulation, after taking into account a relatively large number of various factors that undoubtedly influence the climate, tried to show how the climate will change with a further increase in the concentration of CO_2 in the atmosphere. It should also be emphasized that in such considerations it is necessary to solve differential equations with initial and boundary conditions. Under the existing conditions, this is impossible, as there are no measurement points in inaccessible places and satellite images cannot supplement this. Unknown data cannot be replaced by data obtained by averaging, since averaging physical quantities with nonlinear dependencies present in the issue at hand must lead to large errors. Thus, **the results from the computer models used, regardless of the quality of the equipment used and the programs used, cannot be taken seriously**.

Climatologists very often refer to works considered fundamental in discussions. Among them belongs the work [39]. In it, the author discusses the physics of the interaction of "long-wave" radiation with molecular gases. He then presents a "plate" model of the atmosphere. This model somewhat resembles the eight-layer model presented in Chapter 4, but the author ignores the experimental fact of dividing the Earth's thermal radiation into radiation absorbable by CO_2 and radiation not absorbable by this gas. Without any experimental or analytical evidence, the author concludes that the „*In some cases continua result from the overlap of nearby lines, but in other cases continua appear where no lines are in the vicinity.*" Thus, it is assumed without proof that thermal radiation from the entire spectral range is absorbed by CO_2. Of course, one must agree with the author in stating that „*The intricate variation of absorption with frequency makes it difficult to efficiently solve the radiative transfer equations. In line-by-line models, the equations are solved separately on a grid of millions of frequencies and the results are summed to obtain net fluxes*". But is it the only way that leads to knowledge of the phenomenon. Why is experimental cognition rejected?

Regarding Ångström's work, the author states that Ångström was wrong, as he *"modern spectroscopy shows that CO_2 is nowhere near being saturated. Ångström's laboratory experiments were simply too inaccurate to show the additional absorption in the wings of the 667-cm^{-1} CO_2 feature that follows upon increasing CO_2"*.

Well, no science, including "modern spectroscopy," can dispute the experimental facts, and these clearly show that the process of absorption of thermal radiation in carbon dioxide with a sufficiently large mass of this gas must saturate. Moreover, in the experiments used by Ångström, saturation was proven on the basis of measuring radiant power without delving into the spectral structure. If one considers these experiments inaccurate due to the low-precision apparatus used at the time, they should be repeated. You can't dismiss experimental facts using theory. One reaches the absurdity attributed to Hegel – *"If the facts contradict the theory, so much the worse for the facts"*.

In the paper [40], based on results from the HITRAN database, a qualitative attempt is made to justify that there is no saturation effect. Meanwhile, Fig. 6a, presented there, clearly shows that this effect is present. As the concentration of CO_2 in the atmosphere

increases, the radiative forcing increases more slowly with the increase in this concentration. The author tries to prove that this increase is logarithmic and therefore saturation cannot occur. With the logarithmic growth can be agreed but only for a certain range of concentrations, because assuming in the considered range of pressures the shape of the oscillation-rotation lines described by the Lorentz function, it can be seen that indeed first the top of the line saturates and only then its wings, and as a result the line at saturation widens. However, this condition will occur when the lines as a result of broadening are not yet overlapping. Later on, the spectrum will be banded and the shape of the band will be described by the distribution of the occupancy of the rotational levels and, as a result, an increase in CO_2 concentration will no longer affect the width of the band. The article does not state whether these phenomena were taken into account, and therefore it is difficult to comment on the results presented. What is known, however, is that these are theoretical results and cannot contradict the facts shown in the experiments conducted. In addition, results for very high concentrations of CO_2 in the Earth's atmosphere are given in the article in an abstract way that is completely detached from reality.

In the paper [42], based, among other things, on the previous literature items discussed, the author claims that the absorption of thermal radiation of the Earth, is currently not fully saturated. In further considerations, the author ultimately does not deny the occurrence of radiation absorption saturation, but, like the authors of many other works [43, 44], he claims that with an increase in CO_2 concentration in the atmosphere, radiation emission shifts to higher layers, where the temperature is lower. This reasoning is corrected in Chapter 3 of this paper. There it is shown that, assuming the experimentally proven version of saturation, one automatically assumes a division of thermal radiation into radiation absorbable by CO_2 and radiation nonabsorbable by this gas. Thus, no matter in which layer of the atmosphere the radiation from CO_2 is emitted, the nonabsorbable radiation will not decrease, and thus the decrease in the emission of thermal radiation to space as a function of the concentration of CO_2 in the atmosphere must be saturated.

An interesting study is [24]. The authors, analyzing very carefully the spectra of thermal radiation coming from Earth from spectrometers placed on satellites, at intervals of nearly three decades, examined the impact of various greenhouse gases on the decrease in brightness temperature, which is closely related to radiance and thus to radiative forcing. It can therefore be concluded that work based on direct measurements unequivocally determines the impact of increased CO_2 concentrations in the atmosphere on the decrease in infrared radiation emitted into space, which cools our planet. It is a pity that the authors focused only on brightness temperature, exaggerating the significance of its minimal decrease. A slightly more detailed analysis carried out in subsection 2.4 shows that **despite the alarming increase in CO_2 concentration during the period under consideration, there was virtually no significant reduction in the intensity of infrared radiation emitted into space as a result, and ultimately the increase in CO_2 concentration did not cause an increase in the Earth's temperature**.

The paper [1] describes in detail the results of measurements and analyses from completed ice sheet drilling at Vostok Station in East Antarctica. This provided information on, among other things, atmospheric composition and air temperature during the last four glacial-interglacial cycles. It was shown that throughout the record, atmospheric concentrations of carbon dioxide and methane correlate well with air temperature in Antarctica. The authors, probably realizing that it does not necessarily follow from the fact that two events occur at the same time that one is the cause of the other, cautiously put forward only a hypothesis about climate change over the time interval under consideration. They suggest that during any end of the glacial period there may have been orbital forcing with a possible contribution from local insolation changes and then two strong amplifiers may have acted, first greenhouse gases and then deglaciation and ice-albedo feedback. A suggestion is also made about the role of the ocean in regulating long-term changes in atmospheric CO_2 concentration. It should be noted that in this work as well as in other works on glacier drilling and also geological survey work, studies are made on relatively long time periods. Therefore, it is impossible in these works to determine the order of the increase in air temperature and the increase in atmospheric CO_2 concentration as shown in the work [37], that the temperature increases first and thus it must be the cause of the increase in CO_2 concentration, and not vice versa.

In summary, it should be noted that "important" climatological studies on the atmospheric impact of carbon dioxide on atmospheric temperature do not take into account the experimentally demonstrated division of Earth's thermal radiation into radiation absorbable by CO_2 and radiation not absorbable by this gas.

It should be noted that this work does not concern climate, but only the interaction of thermal radiation with carbon dioxide in the atmosphere.

The conclusions drawn from this study are consistent with the findings presented by Professor W.J. Witteman, a renowned expert in the physics of infrared radiation interaction with CO_2 molecules [45], who clearly demonstrated that "The absorption of surface radiation by the current CO_2 concentration is practically saturated, so an increase in the CO_2 concentration cannot enhance the greenhouse effect".

Acknowledgements

We would like to thank the Management Board of the Lower Silesia Region, NSZZ Solidarność, MOZ NSZZ “Solidarność” Beko Poland Manufacturing Sp. z o.o. Branch in Wrocław and MOZ NSZZ “Solidarność” PKP S.A. with its registered office in Wrocław for financial support of the issue.

Literature

[1] PETIT J.R., JOUZEL J., RAYNAUD D. et al., *Climate and atmospheric history of the past 420,000 years from the Vostok ice core, Antarctica*, Nature, 1999, Vol. 399, pp. 429–436, https://www.nature.com/articles/20859

[2] ARRHENIUS S., *On the Influence of Carbonic Acid in the Air upon the Temperature of the Ground*, Philosophical Magazine and Journal of Science Series 5, April 1896, Vol. 41, pp. 237–276.

[3] ÅNGSTRÖM K., *Über die Bedeutung des Wasserdampfes und der Kohlensäure bei der Absorption der Erdatmosphäre*, Annalen der Physik, Vierte Folge, 1900, Band 3, 12. Heft, S. 720–732.

[4] KUBICKI J., KOPCZYŃSKI K., MŁYŃCZAK J., *Saturation of the absorption of thermal radiation by atmospheric carbon dioxide*, IAPGOŚ, 2020a, Vol. 10, 77–81, http://doi.org/10.35784/iapgos.826

[5] KUBICKI J., KOPCZYŃSKI K., MŁYŃCZAK J., *Absorption characteristics of thermal radiation for carbon dioxide*, IAPGOŚ, 2022, Vol. 3, pp. 4–7, https://doi.org/10.35784/iapgos.2998

[6] *Efekt cieplarniany – ABC*, 25 października 2021, https://naukaoklimacie.pl/aktualnosci/efekt-cieplarniany-abc

[7] PIERREHUMBERT R.T., *Infrared radiation and planetary temperature*, Physics Today, 2011, 64 (1), 33–38, DOI: 10.1063/1.3541943, https://physicstoday.aip.org/features/infrared-radiation-and-planetary-temperature

[8] KOCHKOV D. et al., *Neural general circulation models for weather and climate*, Nature, 2024, Vol. 632, pp. 1060–1066, https://www.nature.com/articles/s41586-024-07744-y

[9] MANABE S., WETHERALD R.T., *On the Distribution of Climate Change Resulting from an Increase in CO_2 Content of the Atmosphere*, Journal of the Atmospheric Sciences, Jan 1980, Vol. 37, Issue 1, https://doi.org/10.1175/1520-0469(1980)037<0099:OTDOCC>2.0.CO;2

[10] MITCHELL J.F.B., *The "Greenhouse" effect and climate change*, Reviews of Geophysics, February 1989, pp. 115–139, https://doi.org/10.1029/RG027i001p00115

[11] ZAINAB M. ABBOOD and OSAMA T. AL-TAAI, *Calculation of absorption and emission of thermal radiation by clouds cover*, ARPN Journal of Engineering and Applied Sciences, December 2018, Vol. 13, No. 24, ISSN 1819-6608.

[12] ALADOS-ARBOLEDAS L., VIDA J., OLMO F.J., *The estimation of thermal atmospheric radiation under cloudy conditions*, International Journal of Climatology, January 1995, Vol 5, Issue 1, pp. 107–116.

[13] SAKURAI A., MARUYAMA S., SEIGO SAKAI, NISHIKAWA O., *The effect of three-dimensional radiative heat transfer in cloud fields using the radiation element method*, Journal of Quantitative Spectroscopy Radiative Transfer, June 2005, Vol. 93, Issue 1–3, pp. 79–87, DOI: 10.1016/j.jqsrt.2004.08.013.

[14] JAIN P.C., *Greenhouse effect and climate change: scientific basis and overview*, Renewable Energy, June–July 1993, Vol. 3, Issues 4–5, pp. 403–420, https://doi.org/10.1016/0960-1481(93)90108-S

[15] TRENBERTH K.E. and FASULL J.T., *Global warming due to increasing absorbed solar radiation*, Geophysical Research Letters, 2009, Vol. 36, L07706, DOI: 10.1029/2009GL037527, 2009.

[16] LANDSBERG H.E., *Man-Made Climatic Changes: Man's activities have altered the climate of urbanized areas and may affect global climate in the future*, Science, 18 Dec. 1970, Vol. 170, Issue 3964, pp. 1265–1274, DOI: 10.1126/science.170.3964.1265.

[17] WILD M., *Decadal changes in radiative fluxesat land and ocean surfaces and their relevance for global Warming*, WIREs Climate Change, Jan. 2016, Vol. 7, Issue 1, pp. 1–159, https://doi.org/10.1002/wcc.372
[18] MADDEN R.A., RAMANATHAN V., *Detecting Climate Change due to Increasing Carbon Dioxide*, Science, 15 Aug. 1980, Vol. 209, Issue 4458, pp. 763–768, DOI: 10.1126/science.209.4458.763.
[19] SHINE K.P., DE FORSTER F.P.M., *The effect of human activity on radiative forcing of climate change: a review of recent developments*, Global and Planetary Change, May 1999, Vol. 20, Issue 4, pp. 205–225.
[20] PALMER T.N., *Nonlinear Dynamical Perspective on Climate Prediction*, European Centre for Medium-Range Weather Forecasts, Shinfield Park, Reading, United Kingdom, (Manuscript received 7 October 1997, in final form 26 February 1998), https://doi.org/10.1175/1520-0442(1999)012<0575:ANDPOC>2.0.CO;2
[21] SHERWOOD B.I., *CO_2-induced global warming: a skeptic's view of potential climate change*, Climate Research Clim Res, Published April 9 1998, Vol. 10, 69–82, https://www.jstor.org/stable/24865955
[22] MANABE S., WETHERALD R.T., *On the Distribution of Climate Change Resulting from an Increase in CO_2 Content of the Atmosphere*, Journal of the Atmospheric Sciences, Jan. 1980, Vol. 37, Issue 1, https://doi.org/10.1175/1520-0469(1980)037<0099:OTDOCC>2.0.CO;2
[23] WARD P.L., American Meteorogical Society, 98th Annual Meeting 2018.
[24] HARRIES J.E., BRINDLEY H.E., SAGOO P.J., BANTGES R.J., *Increases in greenhouse forcing inferred from the outgoing longwave radiation spectra of the Earth in 1970 and 1997*, Nature, 2001, Vol. 410, pp. 355–357.
[25] https://www.renewableenergyworld.com/solar/secretary-steven-chu-announces-departure-accomplishments-in-a-letter-to-energy-department-employees/?utm_source=chatgpt.com
[26] IPCCINTERGOVERNMENTAL PANEL ON Climate Change 2021 The Physical Science Basis, https://www.ipcc.ch/report/ar6/wg1/downloads/report/IPCC_AR6_WGI_SPM_final.pdf
[27] AR6 Synthesis Report: Climate Change 2023, The IPCC finalized the Synthesis Report for the Sixth Assessment Report during the Panel's 58th Session held in Interlaken, Switzerland from 13–19 March 2023, https://www.ipcc.ch/report/sixth-assessment-report-cycle/
[28] SCHILDKNECHT D., *Saturation of the infrared absorption by carbon dioxide in the atmosphere*, International Journal of Modern Physics B, 2020, Vol. 34, No. 30, 2050293.
[29] SCHACK A., *Der Einfluß des Kohlendioxid-Gehaltes der Luft auf das Klima der Welt*, Physikalische Blätter, 1972, Vol. 28. pp. 26–28.
[30] HARDE H., *Radiation and Heat Transfer in the Atmosphere: A Comprehensive Approach on a Molecular Basis*, Int. J. Atm. Sci., 2013, 503727.
[31] PLANCK M., *On the Law of Energy Distribution in the Normal Spectrum*, Annals of Physics, 1901, 4, 553–563.
[32] RYBICKI G.B., LIGHTMAN A.P., *Radiative processes in astrophysics*, Haruard-Smithsonian Center for Astrophysics.
[33] https://www.jpl.nasa.gov/images/pia18833-nasa-spacecraft-maps-earths-global-emissivity/
[34] https://physics.nist.gov/cgi-bin/cuu/Value?sigma
[35] HAMMEL E., STEINER M., MARVAN C. et al., *CO_2 Back-Radiation Sensitivity Studies under Laboratory and Field Conditions*, Atmospheric and Climate Sciences, October 2024, Vol.14, No.4.
[36] MARKOWICZ K., *Procesy radiacyjne w atmosferze*, Materiały do wykładu, Instytut Geofizyki, Wydział Fizyki, Uniwersytet Warszawski.
[37] HUMLUM O., STORDAHL K., SOLHEIM J., *The phase relation between atmospheric carbon dioxide and global temperature*, Global and Planetary Change, 2013, 100, 51–69.
[38] WITTEMAN W.J., *The CO_2 Laser*, Springer-Verlag, Berlin–Heidelberg Gmbh, https://link.springer.com/content/pdf/10.1007/978-3-540-47744-0.pdf

[39] PIERREHUMBERT R.T., *Infrared radiation and planetary temperature*, Physics Today, 2011, 64 (1), 33–38, https://doi.org/10.1063/1.3541943
[40] ZHONG W., HAIGH J.D., *The greenhouse effect and carbon dioxide*, Weather, Apr. 2013, Vol. 68, Issue 4, pp. 86–98, i–iv, 99–112, E1–E2, https://doi.org/10.1002/wea.2072
[41] DIEHL W.S., *Standard Atmosphere: Tables and Data*, US Government Printing Office, 1925, https://ntrs.nasa.gov/api/citations/19930091285/downloads/19930091285.pdf
[42] EYMET V., CREVOISIER C., GRANDPEIX J., *Greenhouse Effect: The Relative Contributions of Emission Height and Total Absorption*, Journal of Climate, 01 May 2020, Vol. 33, Issue 9, pp. 3827–3844.
[43] DUFRESNE J. at el., *Greenhouse Effect: The Relative Contributions of Emission Height and Total Absorption*, Journal of Climate, 01 May 2020, Vol. 33, Issue 9, https://doi.org/10.1175/JCLI-D-19-0193.1
[44] RAPP D., *How Increased CO_2 Warms the Earth-Two Contexts for the Greenhouse Gas Effect*, IgMin Research, 2024, 2 (10), DOI: 10.61927/igmin259
[45] WITTMAN W.J., *Global warming by thermal absorption of CO_2*, 2023, https://www.clepair.net/witteman-CO2+IR.pdf

Experimental study of the effect of increased CO_2 concentration on infrared radiation absorption

The aim of this study was to experimentally investigate the effect of CO_2 concentration in a gas mixture corresponding to the Earth's atmosphere on radiative forcing and to analyze the saturation of this phenomenon. The results of the research do not concern the analysis of climate change on Earth, but draw attention to the importance of this issue in determining the credibility of the scientific basis of the so-called "Green Deal". The second chapter presents published experimental facts and theoretical justification for carbon dioxide saturation of Earth's thermal radiation absorption and radiative forcing under current conditions. In chapter three, a single-layer model is used to present an interpretation of the facts described, which unequivocally confirm the saturation discussed. The fourth chapter presents an original eight-layer model along with a description of the measurement system that allows experimental data for this model to be determined. The analysis provided a quantitative picture of the interaction between Earth's thermal radiation and carbon dioxide in the atmosphere and fully confirmed the results obtained earlier. The summary refers to leading works in the field of climatology that deny the described saturation processes. Attention is drawn to the erroneous assumptions made in these works.

Key words: CO_2, infrared radiation absorption, greenhouse gases, carbon dioxide saturation of thermal radiation absorption

WUST Publishing House prints
can be obtained via mailorder:
zamawianie.ksiazek@pwr.edu.pl
ksiegarnia.pwr.edu.pl

ISBN 978-83-8134-019-9